



Energy, Mines and
Resources Canada

Énergie, Mines et
Ressources Canada

Earth Physics Branch

Direction de la physique du globe

1 Observatory Crescent
Ottawa Canada
K1A 0Y3

1 Place de l'Observatoire
Ottawa Canada
K1A 0Y3

Geothermal Service of Canada

Service géothermique du Canada

DETECTION OF PERMAFROST BASE IN THICK PERMAFROST AREAS -
TRANSIENT ELECTROMAGNETIC SURVEY IN MACKENZIE DELTA AREA, N.W.T.

GEO-PHYSI-CON Co. Ltd.
Calgary, Alberta

Earth Physics Branch Open File Number 83-17
Dossier public de la Direction de la Physique du Globe No. 83-17
Ottawa, Canada

NOT FOR REPRODUCTION

REPRODUCTION INTERDITE

Department of Energy, Mines &
Resources Canada
Earth Physics Branch
Division of Gravity, Geothermics
and Geodynamics

Ministère de l'Énergie, des
Mines et des Ressources du Canada
Direction de la Physique du Globe
Division de la gravité, géothermie
et géodynamique

77 Pages
Price: \$22.00

This document was produced
by scanning the original publication.

Ce document est le produit d'une
numérisation par balayage
de la publication originale.

GEO-PHYSI-CON

DETECTION OF PERMAFROST BASE IN
THICK PERMAFROST AREAS
TRANSIENT ELECTROMAGNETIC SURVEY
MACKENZIE DELTA AREA, N.W.T.

Prepared For

ENERGY, MINES AND RESOURCES
EARTH PHYSICS BRANCH
DIVISION OF GRAVITY, GEOTHERMAL AND GEODYNAMICS

Prepared By

GEO-PHYSI-CON CO. LTD.
CALGARY, ALBERTA

June 1983
C83-12

TABLE OF CONTENTS

	Page
1.0 INTRODUCTION	1
2.0 LOGISTICS	2
3.0 DATA ACQUISITION	4
4.0 INSTRUMENTATION AND THEORY	6
4.1 EM37 - Transient System	6
4.2 EM31 and EM34-3 - Fixed Frequency Systems	19
5.0 INTERPRETATION METHODS	22
5.1 General	22
5.2 Relative and Absolute Coordinates	23
5.3 The Description of Apparent Resistivity Curves	23
5.4 The Distortions of the Apparent Resistivity Curves	28
5.5 Fixed Frequency EM Data	29
6.0 RESULTS	29
6.1 Taglu Site	30
6.2 Parsons Lake	35
7.0 CONCLUSIONS AND RECOMMENDATIONS	36
APPENDIX A - Manufacturer's Specifications for Geonics EM31, EM34-3 and EM37	

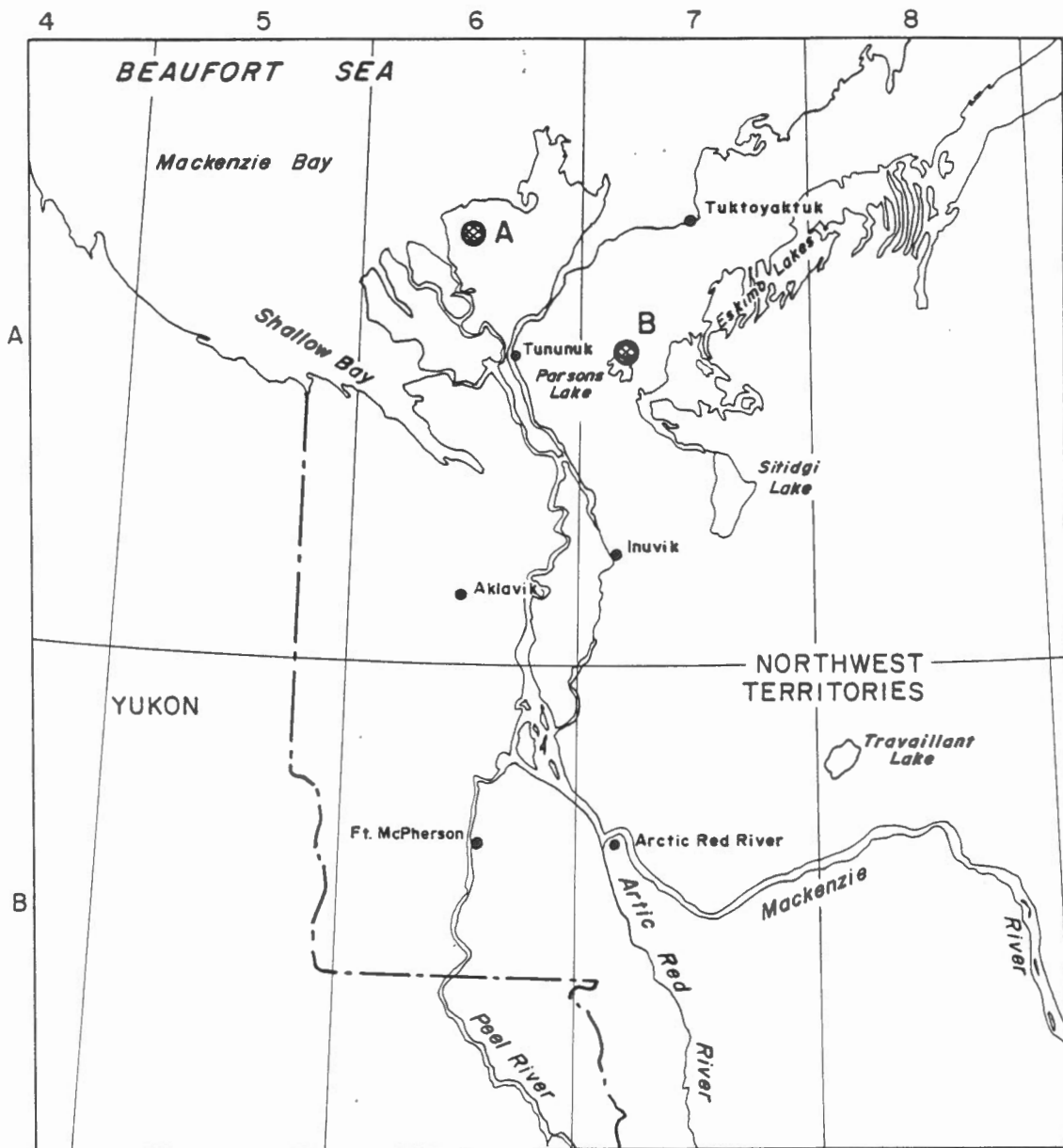
1.0 INTRODUCTION

During March, 1983 a geophysical test survey was performed at two sites on land near Tuktoyaktuk, N.W.T. The test survey was conducted using the methods of transient electromagnetic soundings and fixed frequency electromagnetic induction at low induction number. The objective of the survey was to determine the variation in depth to and the total thickness of permafrost in the vicinity of previously drilled oil wells for which ground thermal measurements were available.

Figure 1 shows the general locations of the two sites investigated. Figures 2 and 3 show the exact locations of the survey lines at the Taglu and Parsons Lake fields, respectively.

The field work was undertaken in conjunction with a similar offshore survey performed for Energy, Mines and Resources, Geological Survey of Canada. The two surveys ran concurrently to take advantage of mobilization and demobilization expenses and efficient helicopter utilization.

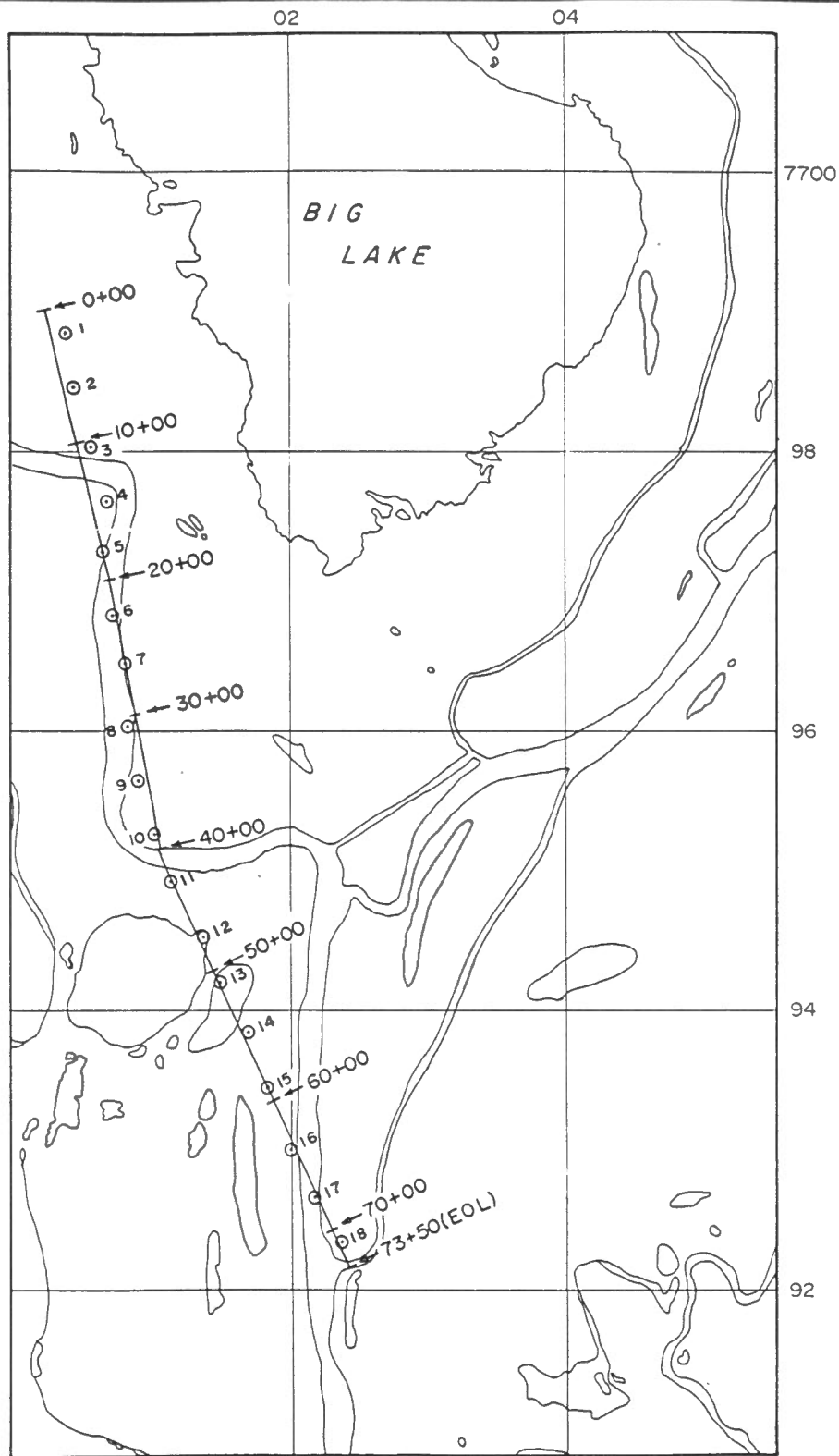
A report detailing the logistics and data acquisition stages of the project and a preliminary appraisal of the data was



- A Taglu Site
- B Parsons Lake Site

EARTH PHYSICS BRANCH SITE LOCATION MAP

	SCALE 1: 2,500,000	DRAWN BY B.T.	DATE May, 1983
	N.T.S.	PROJECT NO. C 83-12	FIGURE 1



SCALE (metres)



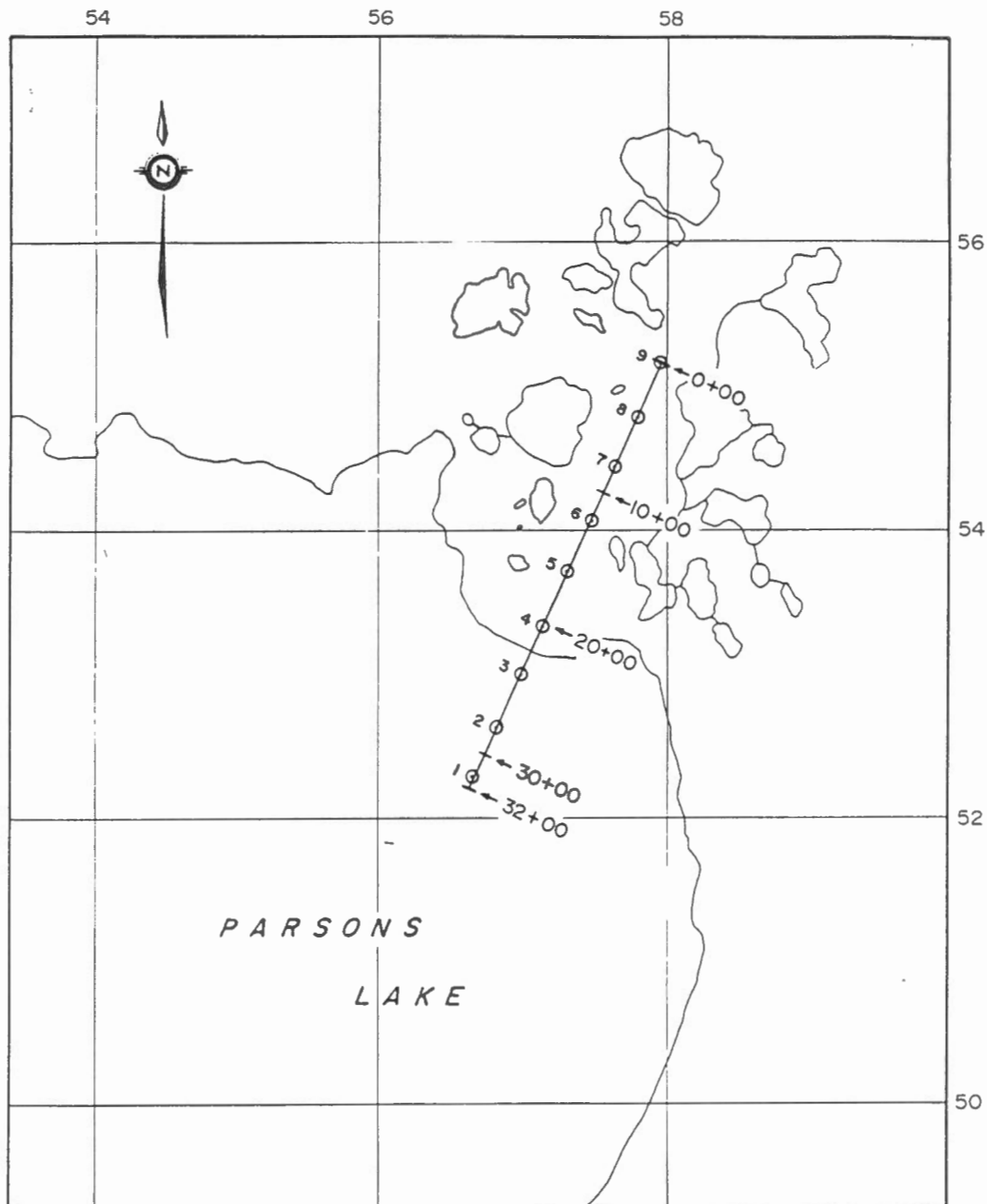
LEGEND

- ← 0+00 EM Line Chainage
- ⊙ 2 TEM Loop Centre

EARTH PHYSICS BRANCH
SITE LOCATION MAP
TAGLU FIELD

GEO-PHYSICON

SCALE 1:50,000	DRAWN BY D.T.	DATE Mar., 1983
N.T.S. 107 C/6 W	PROJECT NO C83-12	FIGURE 2



SCALE (metres)



LEGEND

- ← 0+00 EM Line Chainage
- 2⊙ TEM Loop Centre

EARTH PHYSICS BRANCH
SITE LOCATION MAP
PARSONS LAKE

<i>GEO-PHYSICON</i>	SCALE 1:50,000	DRAWN BY D. T.	DATE Mar., 1983
	NTS 107C/2W 107B/15W	PROJECT NO C83-12	FIGURE 3

previously submitted in March, 1983. This report contains detailed descriptions of the transient system and interpretive methods used. The interpreted sections are presented for each of the two sites surveyed. Conclusions regarding the application of transient soundings for mapping of the base of deep permafrost and recommendations concerning the use of the systems for future surveys are discussed.

The work was carried out under DSS Contract Serial Number OSQ 82-00256, dated February 23, 1983. Dr. A. Judge, Earth Physics Branch, Division of Gravity, Geothermal and Geodynamics was the project authority.

2.0 LOGISTICS

The test survey was performed by a four man crew during the periods March 9 to 19 and March 24 to 27, 1983. Mobilization and demobilization between Tuktoyaktuk and Calgary took place on March 8 and 28. Other time was spent performing a similar test survey at two off-shore sites for Energy, Mines and Resources, Geological Survey of Canada.

Crews travelled to and from the survey sites daily by helicopter. Generally, four sling loads were required for each move of the equipment.

Nordik Skidoos were used to lay out and take up cable and to move the generator, transmitter and receiver for the TEM work at each site. Over the course of the survey, 27 stations (approximately 11km) were surveyed at two loop sizes.

All fixed frequency EM measurements were recorded by the crew progressing by snowshoe. About 11 kms of EM survey at 50m and 100m spacings and six effective depths of exploration were recorded.

Accommodations were supplied by Polar Continental Shelf Project (PCSP) at Tuktoyaktuk base camp for the work at Taglu. Helicopter support was provided by Quasar Aviation Ltd. on contract to PCSP. Accommodations for the work in the Parsons Lake area were arranged by Geo-Physi-Con in Inuvik. Helicopter support was supplied by Okanagan Helicopters Ltd. on charter to PCSP.

3.0 DATA ACQUISITION

At each of the sites surveyed measurements using the TEM method were recorded at stations separated by 400m intervals. At each station soundings were performed for transmitter loop sizes of 400m by 400m and 100m by 100m. The large loop size was used to gather data identifying the base of permafrost at each station. The small loop size was used to identify lateral discontinuities and complex layering that were less well evidenced in the large loop data.

At each site EM measurements were taken along a line intersecting the TEM stations. EM data was gathered using six different measurement modes. Table 1 lists the exploration modes, station spacing and effective depths of exploration.

At the Big Lake site (Taglu field) 18 stations were placed along a line as shown in Figure 2. This line lies approximately 200m to 300m west of the line proposed. Snow depths at this site were generally in the order of 1m. Snow was hard packed at the north end of the line but became looser and deeper at the southern end of the line. It was not possible to lay out and take up cable by Skidoo past station 18 at the south end of the line.

TABLE 1 - EM MEASUREMENT MODES RECORDED

MEASUREMENT MODE	STATION SPACING	EFFECTIVE EXPLORATION DEPTH
EM31VG - vertical coplanar loop mode at ground level	50 m	2.0
EM31HZ - horizontal coplanar loop mode at hip level	50 m	4.0
EM31HG - horizontal coplanar loop mode at ground level	50 m	5.0
EM34-20V - vertical coplanar loop mode, 20m loop separation	100 m	11.5
EM34-40V - vertical coplanar loop mode, 40m loop separation	100 m	23.0
EM34-40H - horizontal coplanar loop mode, 40m loop separation	100 m	50.0

- 5 -

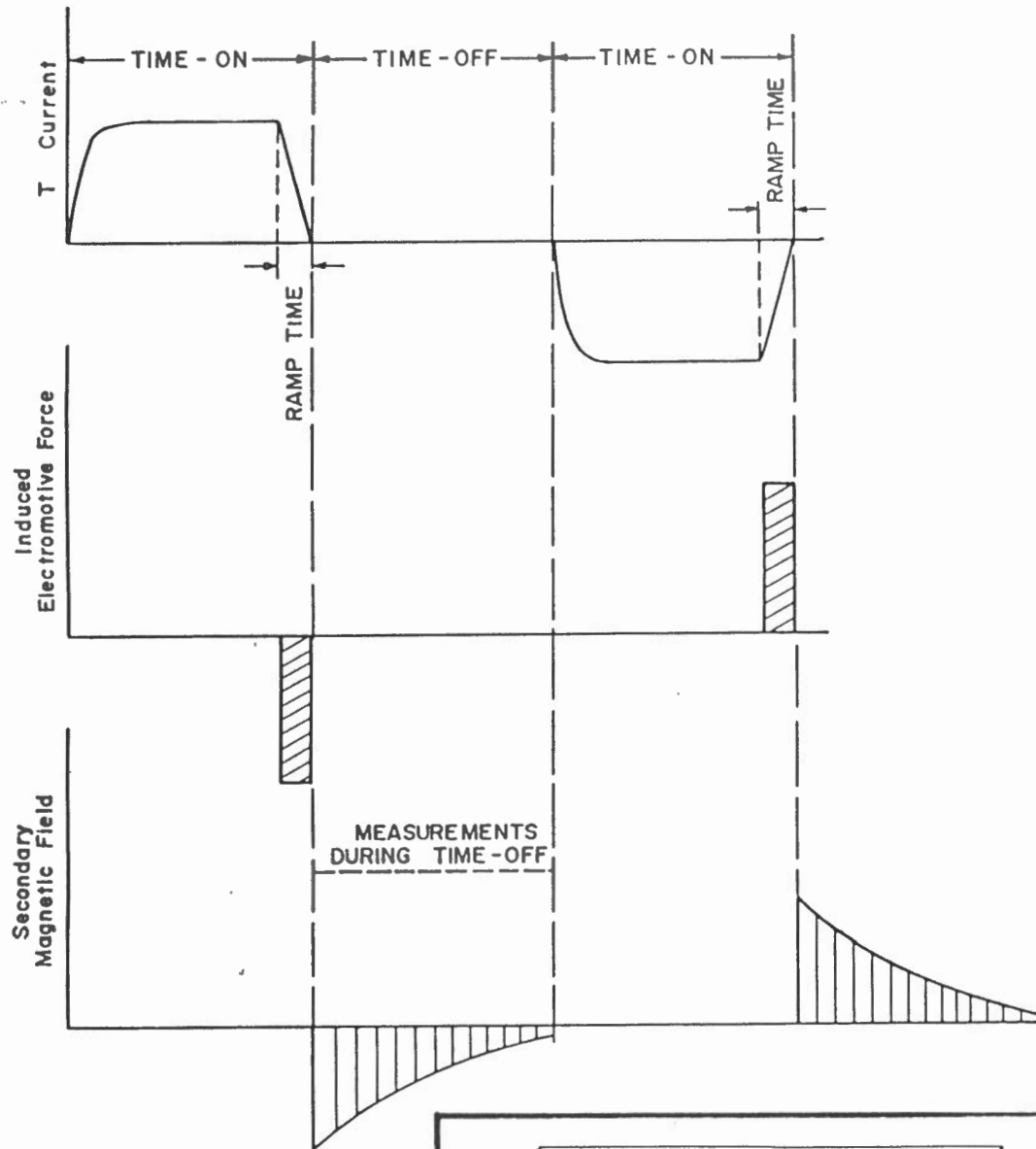
GEO-PHYSI-CON

At the Parsons Lake site 9 stations were placed along the line, as shown in Figure 3. This line follows identically the line proposed for the survey. Snow depths on shore at this site were in the order of 1m. Snow was hard packed and slopes gentle south of station 9. Loose snow and steeper slopes north of station 9 made it impossible to traverse this area by Skidoo.

4.0 INSTRUMENTATION AND THEORY

4.1 EM37 - Transient System

The transient system consists of a transmitter and receiver. The transmitter configuration used was a horizontal non-grounded loop. Figure 4 shows the behavior of the current wave form in the transmitter loop as a function of time. The system has equal periods of time-on and time-off. Three base frequencies for pulse repetition, 30 Hz (HF), 3 Hz (LF) and 0.3 HZ (VLF) can be employed. This gives time-on and time-off periods of 8.33 ms, 83.3 ms and 833 ms, respectively. The turn-on pulse is approximately of the form:



a) CURRENT IN TRANSMITTER LOOP

b) INDUCED ELECTROMOTIVE FORCE CAUSED BY T CURRENT

c) SECONDARY MAGNETIC FIELD CAUSED BY EDDY CURRENTS

GEO-PHYSI-CON

SYSTEM WAVEFORMS

$$J(t) = J_0(1 - \exp(-t/\tau_0))$$

where $J(t)$ is the current at time t after turn-on,
 J_0 is the peak current, and
 τ_0 is an on-time constant.

The time constant τ_0 depends mainly on the size of the transmitter loop used and is approximately 0.5 millisecond for a 400 m by 400 m loop.

The turn-off ramp is linear. The ramp time is experimentally measured on the instrument. The ramp time is a function of transmitter loop size and peak current. It varies from approximately 150 microseconds for a 100 m X 100 m loop to 500 microseconds for a 400 m X 400 m loop.

The receiving element is a multi-turn coil that measures the electromotive force caused by the time derivative of the secondary magnetic field. The receiver can occupy stations inside as well as outside the loop. For the present survey, measurements were made only with the receiver in the centre of the transmitter loop and at base frequencies of 30 Hz and 3 Hz.

Table 2 lists the positions and widths of the time gates of the receiver at high, low and very low frequency. The time is in reference to the bottom of the turn-off ramp (see illustration Table 2). To precisely reference the gate locations to the end of the ramp, the ramp time measured on the transmitter is set on the receiver.

Synchronization of the transmitter and receiver is achieved using high stability (oven controlled) quartz crystals. This method of synchronization requires phasing of the crystals each time the transmitter frequency is changed or the transmitter is shut down. During transmitter shut down the oven temperatures are maintained for both the transmitter and receiver using the receiver battery pack.

Detailed manufacturer's specifications on the instrument are given in Appendix A.

4.1.1 Definition of Apparent Resistivity

It is common in electrical and electromagnetic prospecting (especially in soundings) not to work with the behavior of fields, but to convert the measured field components into apparent

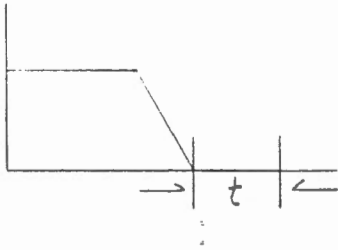


TABLE 2

List of Time of Gate Centres and Gate Widths

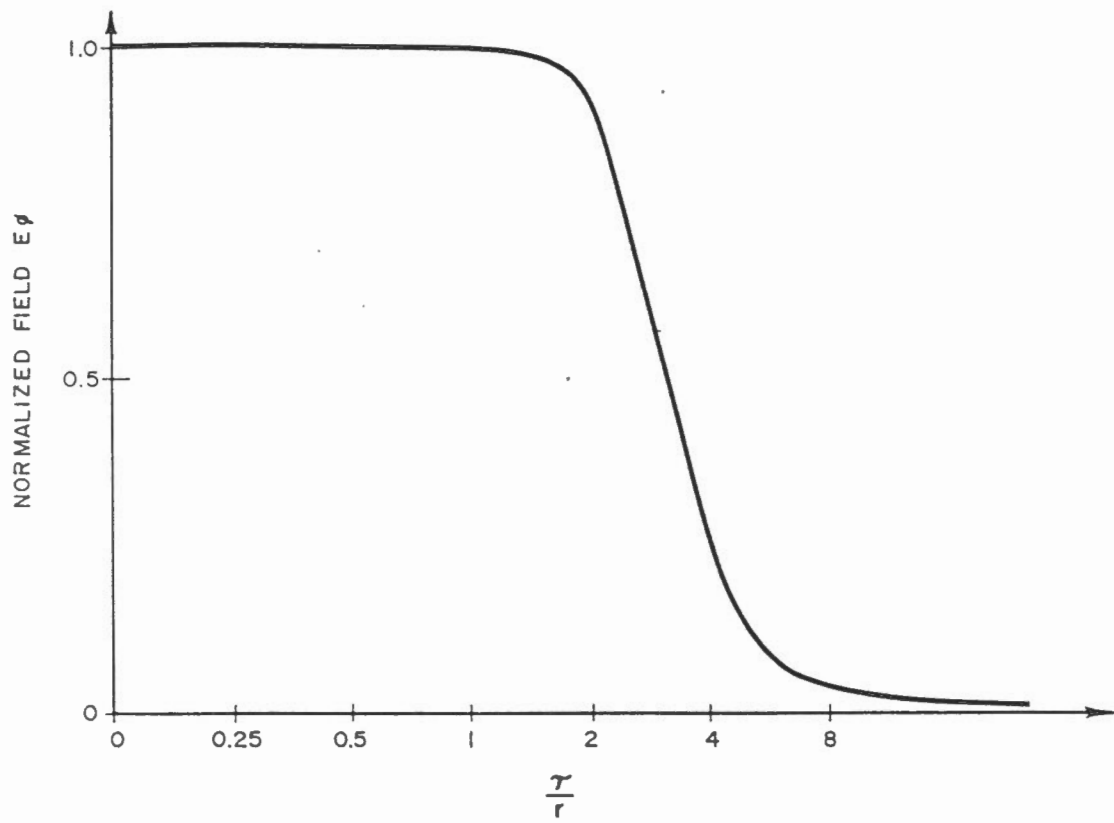
CHANNEL NO.	GATE CENTRE			GATE WIDTH		
	HF	LF	VLF	HF	LF	VLF
1	0.089 ms	0.89 ms	8.9 ms	0.018 ms	0.18 ms	1.8 ms
2	0.100	1.00	10.0	0.024	0.24	2.4
3	0.140	1.40	14.0	0.037	0.37	3.7
4	0.177	1.77	17.7	0.036	0.36	3.6
5	0.220	2.20	22.0	0.050	0.50	5.0
6	0.280	2.80	28.0	0.072	0.72	7.2
7	0.355	3.55	35.5	0.076	0.76	7.6
8	0.443	4.43	44.3	0.100	1.00	10.0
9	0.564	5.64	56.4	0.142	1.42	14.2
10	0.713	7.13	71.3	0.156	1.56	15.6
11	0.881	8.81	88.1	0.180	1.80	18.0
12	1.096	10.96	109.6	0.250	2.50	25.0
13	1.411	14.11	141.1	0.380	3.80	38.0
14	1.795	17.95	179.5	0.390	3.90	39.0
15	2.224	22.24	222.4	0.500	5.00	50.0
16	2.850	28.50	285.0	0.720	7.20	72.0
17	3.600	36.00	360.0	0.780	7.80	78.0
18	4.490	44.90	449.0	1.080	10.80	108.0
19	5.700	57.00	570.0	1.420	14.20	142.0
20	7.190	71.90	719.0	1.560	15.60	156.0

resistivities. This approach has also been used for many years in transient electromagnetic soundings.

It has been shown that the system, consisting of a square transmitter loop with the receiver at its centre, is completely equivalent in the time range employed to a system consisting of a magnetic dipole transmitter and electric dipole receiver. As a result, the theory developed for the latter case above is valid for the system used, provided that the distance between the dipoles is equal to $1/\sqrt{\pi} \cdot L$, where L is the length of a side of the transmitter loop.

To understand the definitions of apparent resistivity used in this report, consider the behavior of the field induced in a homogeneous half-space. In Figure 5 the tangential electrical field component is plotted versus the parameter, \mathcal{T}/r ,

where
$$\mathcal{T} = \sqrt{2\pi\rho t 10^7} \quad [1]$$



GEO-PHYSI-CON

ENGINEERING GEOPHYSICAL CONSULTANTS

BEHAVIOR OF E_ϕ

C83-12

Figure 5

GEO-PHYSI-CON

r = distance between transmitting dipole and point of measurement in metres,

ρ is the resistivity of half-space in ohm-m, and

t is time after turn-off in seconds

The general behavior of the field is a complex function, but it has been shown that at values of $\tau/r < 2$, and at $\tau/r > 10$, simple asymptotic expressions describe the field to good accuracy (5%). At early stage ($\tau/r < 2$) the field is independent of time and the asymptotic expression is given by:

$$E_{\phi} = \frac{3 m \rho}{2 \pi r^4} \quad [2]$$

where m is the moment of the transmitting dipole in amperes-m².

At late stage ($\tau/r > 10$) the field is given by the expression:

$$E_{\phi} = \frac{m r \mu^{5/2}}{40 \pi^{3/2} \rho^{3/2} t^{5/2}} \quad [3]$$

where μ is magnetic susceptibility of free space in henry/m.

Clearly, two different definitions of apparent resistivity can be introduced from equations 2 and 3, i.e.

early stage definition [4]

$$\rho = \frac{2\pi r^4}{3m} E_{\theta}$$

late stage definition [5]

$$\rho = \frac{\mu}{4\pi t} \left(\frac{r\mu m}{5t E_{\theta}} \right)^{2/3}$$

For the present work it was found convenient to use the late stage expression for apparent resistivity. This is due to the fact that late stage behavior appears relatively quickly in the resistive onshore environments surveyed. Early stage behavior is only observed where near surface sediments are extremely conductive (offshore environments).

The interpretation of transient data mainly consists of comparing the measured apparent resistivity curves to curves computed for certain models of horizontally layered geoelectric sections. For this work, many theoretical apparent resistivity

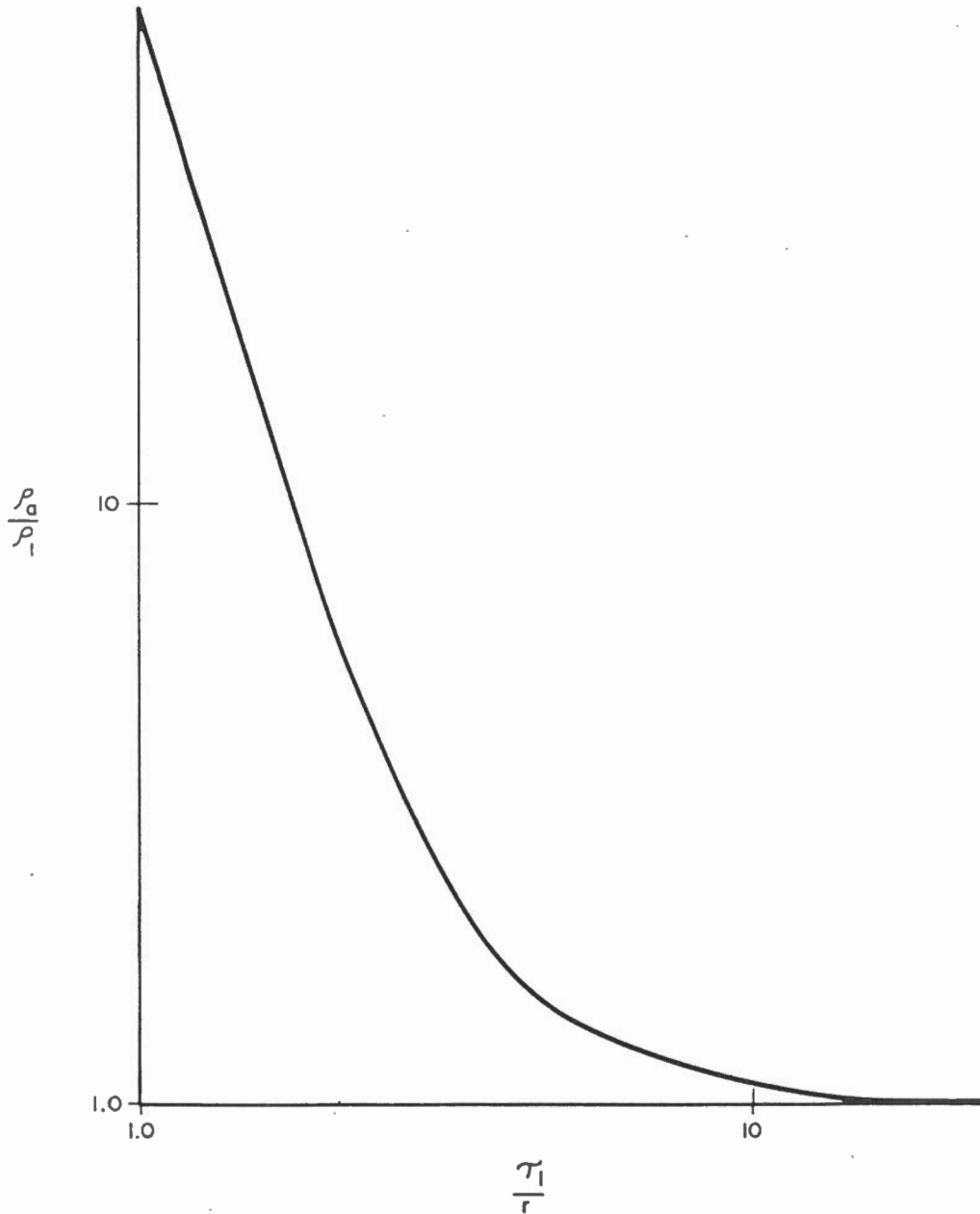
GEO-PHYSI-CON

curves were calculated using specially developed computer programs. The algorithms of the computer programs are subject to the following assumptions:

- a) the half-space is horizontally layered
- b) the current in the transmitting dipole is a perfect step function

To understand the behavior of the apparent resistivity curves generated by using the definition of equation 5, consider the two examples given in Figures 6 and 7. Figure 6 is for homogeneous half-space of resistivity ρ_1 ; on the vertical axis is plotted the ratio of ρ_a/ρ_1 and on the horizontal axis the parameter τ_1/r . It can be seen that when $\tau_1/r > 10$, ρ_a/ρ_1 approaches 1, i.e. the apparent resistivity measured approaches the true resistivity of the half-space. In practice measurements are made at constant r . The true resistivity is measured when

$$t > \frac{r^2}{2 \pi \rho 10^5}$$



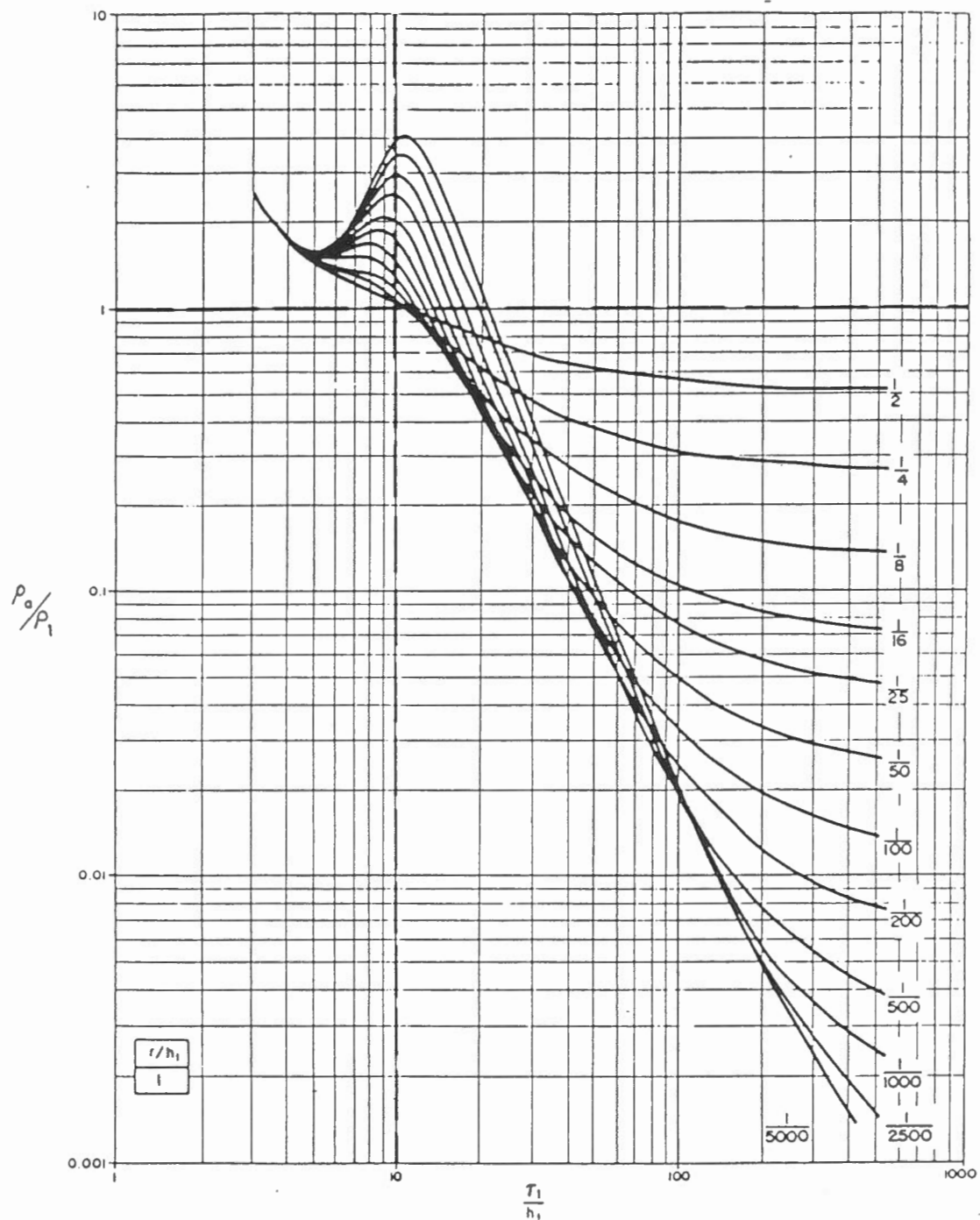
GEO-PHYSI-CON

ENGINEERING GEOPHYSICAL CONSULTANTS

MASTER CURVE
HOMOGENEOUS HALF-SPACE

C83-12

Figure 6



GEO-PHYSI-CON

ENGINEERING GEOPHYSICAL CONSULTANTS

MASTER CURVE
TWO-LAYER MEDIUM

C83-12

Figure 7

At values of $\tau/r < 10$, the values of ρ_a/ρ_1 can be seen to rapidly increase with decreasing τ/r . This is caused by the fact that the field, E_0 , at early time can no longer be described by the late stage asymptotic expression of equation 3. However, it can be expressed using the early stage asymptotic expression of equation 2.

Figure 7 shows late stage apparent resistivity curves for two layer sections when $\rho_2/\rho_1 < 1$. The resistivity stratification for the curves in Figure 7 could, for example, represent frozen ground underlain by unfrozen ground. On the horizontal axis, the parameter τ_1/h_1 is plotted, where h_1 is the thickness of the first layer (frozen ground). The main features of the apparent resistivity curves are:

- a) At small values of the abscissa all curves merge into one corresponding to the behavior of uniform half-space of resistivity, ρ_1 .
- b) At values of $8 < \tau_1/h_1 < 10$, the apparent resistivity curves for sections with $\rho_2/\rho_1 < 1/16$ and $r/h_1 \leq 1$ have a maximum.

- c) At values of $\tau_1/h_1 > 10$, there are descending branches.
For values of $\rho_2/\rho_1 < 1/16$ the descending branches have parallel segments.

- d) At large values of τ_1/h_1 , the apparent resistivity curves approach ρ_2 .

4.1.2 Correction Factors for Ramp Time

It was stated in Section 4.1.1 that the master curves are computed for a perfect step function. The transmitter current when turned off has a finite ramp time (Section 4.1). To make the measured apparent resistivity curve correspond to the master curves a correction must be made for the ramp turn off. The correction factors that are often used are based on either the late stage behaviour of the field or the full expression of the field for a homogenous half-space. In resistive environments (on shore) the late stage expression for the correction is used, as it is valid over the most of the time range employed. In conductive environments (off shore) the correction based on the full field expression is used, as late stage appears more slowly.

GEO-PHYSI-CON

The late stage correction factors are based on the fact that, at late time, the field is proportional to $t^{-5/2}$, so that

$$\frac{Q(t)}{R(t)} = \frac{1}{\Delta T} \int_t^{t+\Delta T} t^{-5/2} dt \quad [6]$$

where $Q(t)$ is the field due to the linear ramp at a time, t ,
 ΔT is the ramp time, and
 $R(t)$ is the field measured due to a perfect step function at time, t .

The full expression correction factor is based on the relation:

$$E_{\phi} = \frac{3m\rho}{2\pi t^4} \left[\phi(u) - \sqrt{\frac{2}{\pi}} u \left(1 + \frac{u^2}{3}\right) e^{-\frac{u^2}{2}} \right] \quad [7]$$

where the parameter $u = \frac{2\pi\rho}{\tau}$,

$\phi(u)$ is the error function,

$$\tau = \sqrt{2\pi\rho t 10^7} \quad ,$$

m is the transmitter dipole moment, and

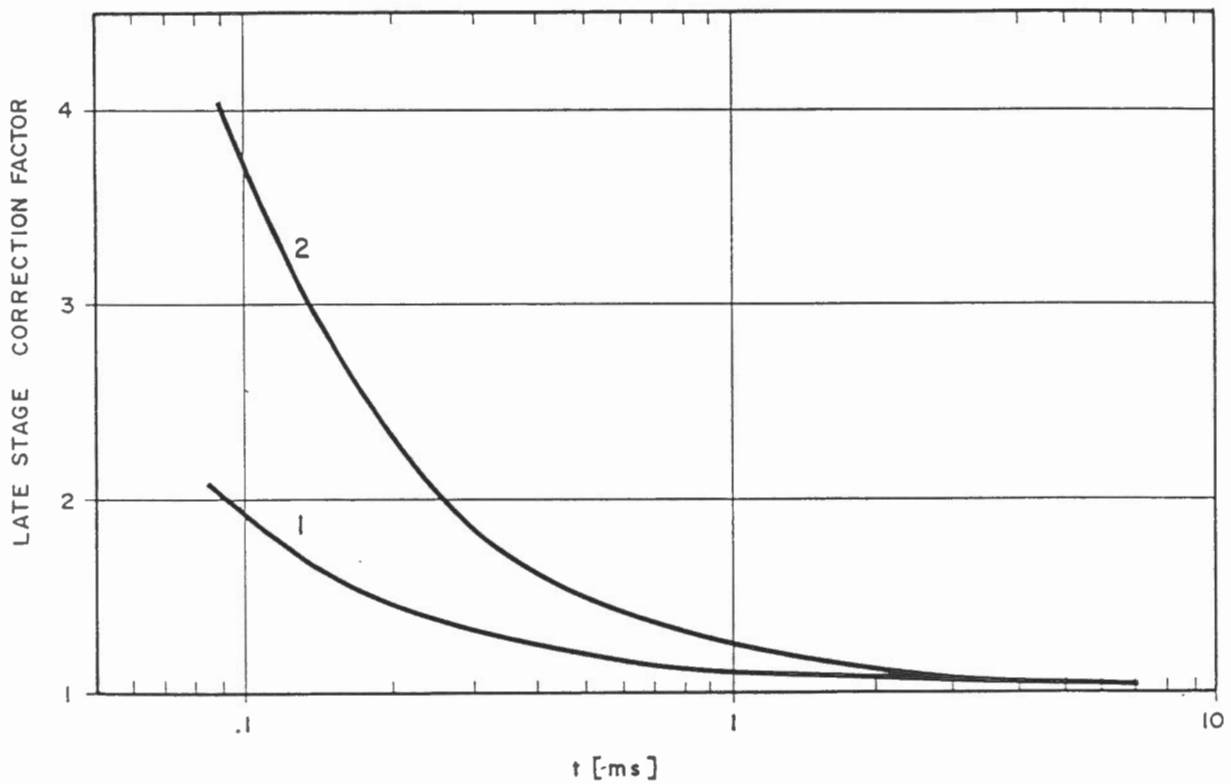
ρ is the half-space resistivity.

In Figure 8 the late stage correction factor is plotted as a function of t for two values of ΔT . In Figure 9 the correction factor based on late stage and on the full expression for the field for a homogeneous half-space having a resistivity of 2 ohm-m are compared. In Figure 10, the difference in apparent resistivities, using the two different correction factors, is shown. The curves merge at the onset of late stage behavior.

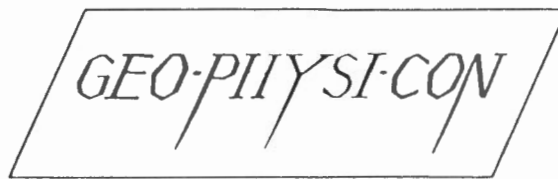
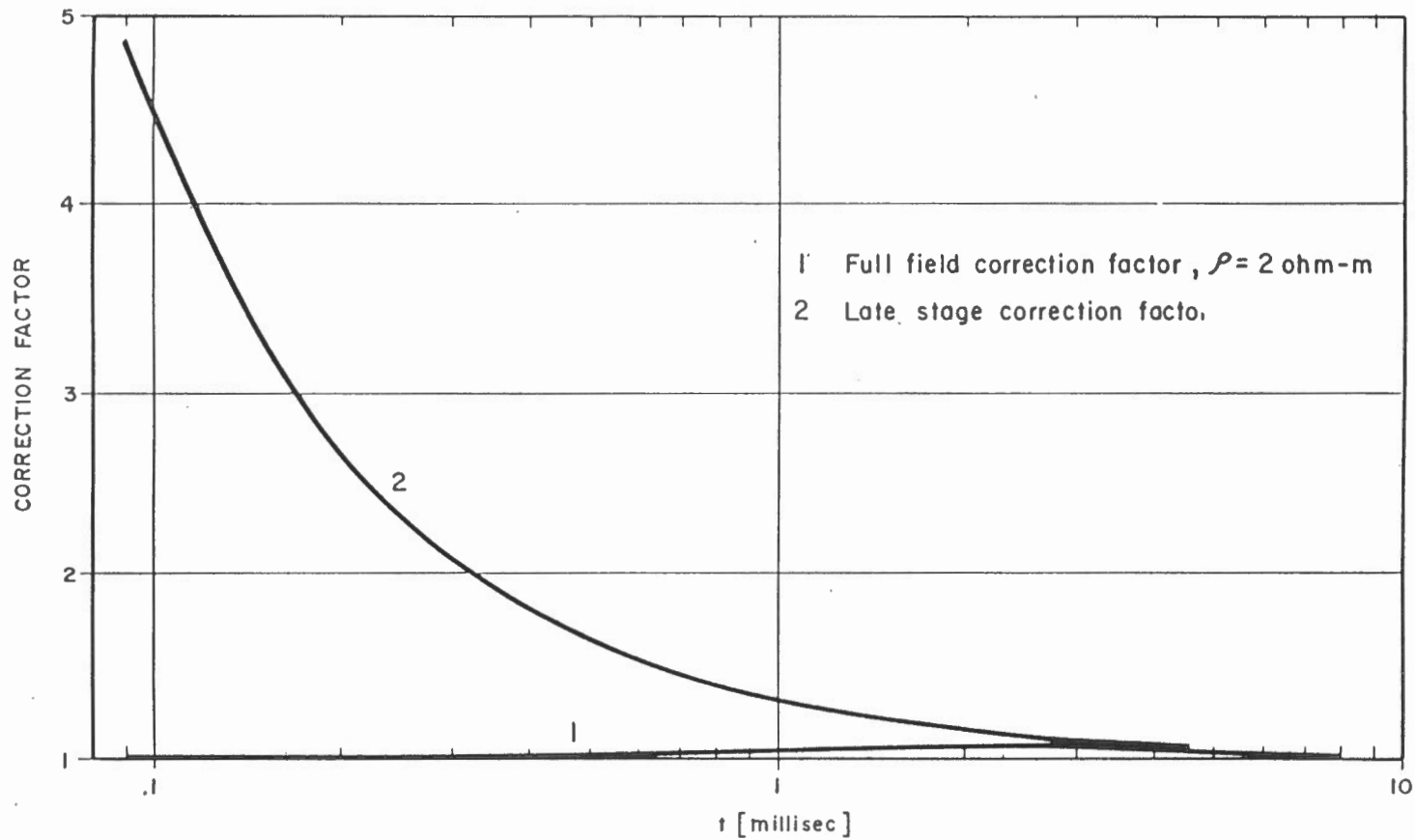
4.1.3 Influence of Turn-on Time and Ramp Time of Previous Pulse

The current waveform in the transmitter loop, as discussed in Section 4.1, consists of periods of time-on and time-off. The electromotive force in the receiver is measured only during time-off. The master curves are computed on the assumption that the secondary field is induced by the last ramp turn-off only. It is assumed that the secondary field, due to previous changes in current, has decayed to a negligible level.

It had been previously found that under certain conditions the turn-on time and ramp turn-off of a previous pulse can influence the measured secondary field. To investigate the influence of previous pulses the following were considered:



- 1 Ramp time 70 microsec
- 2 Ramp time 200 microsec

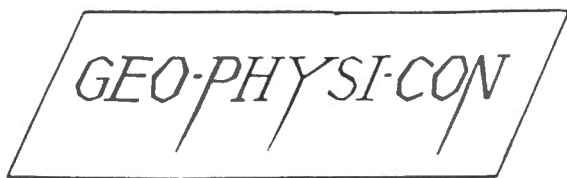
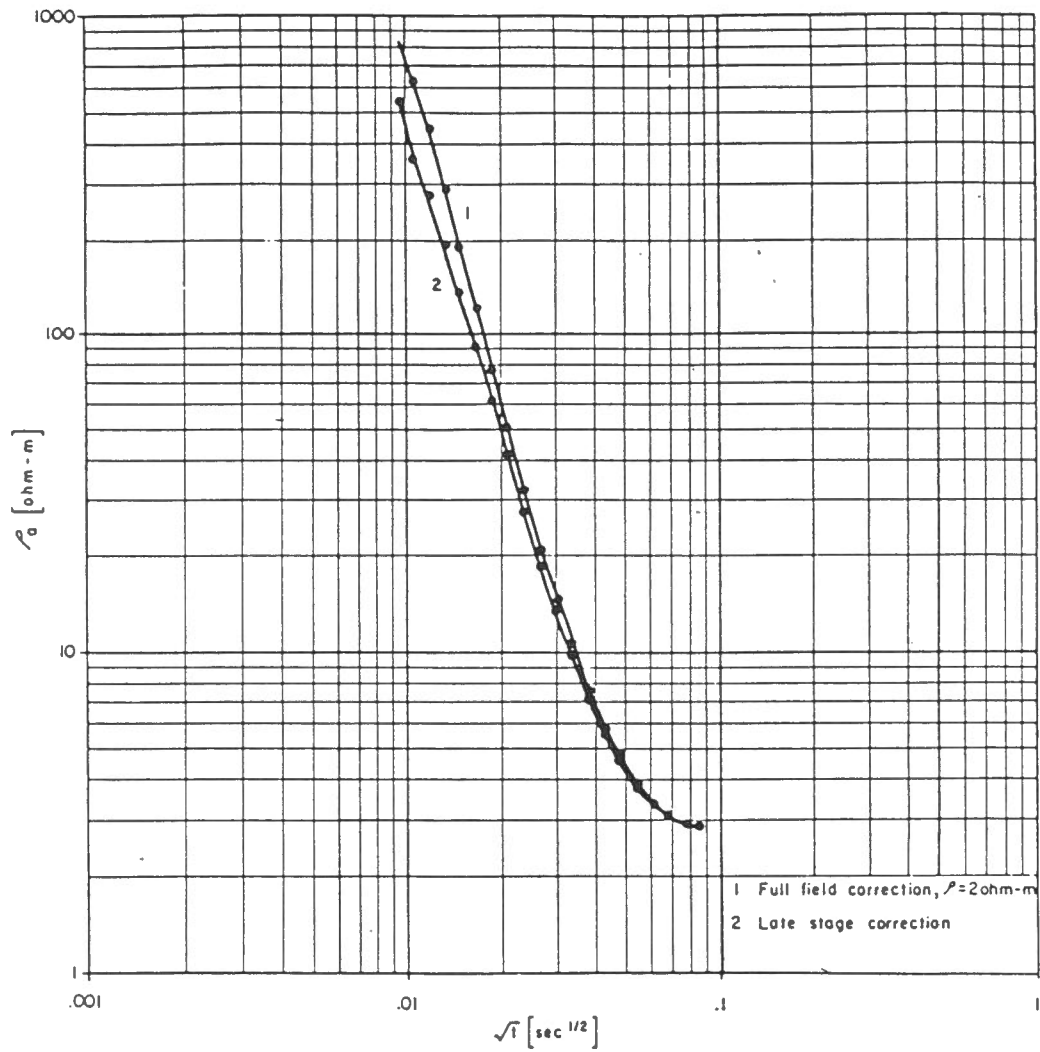


ENGINEERING GEOPHYSICAL CONSULTANTS

CORRECTION FACTORS
 FOR RAMP TIME (250 microsec)

C 83-12

Figure 9



ENGINEERING GEOPHYSICAL CONSULTANTS

APPARENT RESISTIVITY CURVES
 WITH DIFFERENT CORRECTION

C83-12

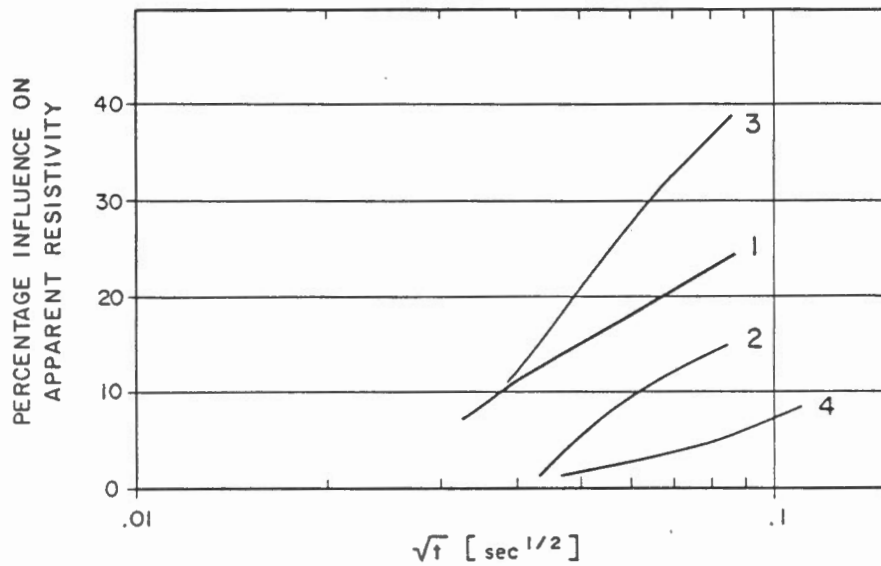
Figure 10

- i) for the field measured at time t the influence of turn-on occurs at $(t+8.3)$ ms for high frequency (HF, 30 Hz), and at $(t+83)$ ms at low frequency (LF, 3 Hz). The polarity of turn-on pulse is opposite in respect to turn-off ramp time.

- ii) the influence of the previous ramp turn-off occurs at $(t+2 \times 8.3)$ ms for high frequency, and at $(t+2 \times 83)$ ms at low frequency. The polarity of this pulse is also opposite to the main turn-off pulse.

- iii) it is assumed that the amplitude of the induced electromotive force is the same for both turn-on and turn-off pulses.

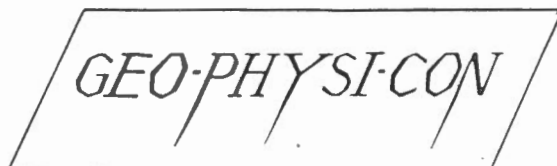
In Figure 11 the influence of the turn-on pulse on the apparent resistivity is computed from master curves for the geoelectric sections typical for onshore permafrost. The computations are made for high and low frequencies. The effect of pulse turn-on can be reduced by measurements at a lower frequency in the same time range, since the last ten time channels at a higher frequency are equivalent to the first 10 time channels at the lower frequency.



ρ_1	h_1	ρ_2	h_2	ρ_3	h_3	ρ_4	h_4	ρ_5
150	50	1000	200	200	150	1000	400	2.5

LEGEND

- 1 Turn-on time for HF
- 2 Previous turn-off time for HF
- 3 Sum of 1 and 2
- 4 Turn-on time for LF



ENGINEERING GEOPHYSICAL CONSULTANTS

INFLUENCE OF SUPERPOSITION OF PULSES FOR ON-SHORE GEOELECTRIC SECTION

©83-12

Figure 11

4.2 EM31 and EM34-3 - Fixed Frequency Systems

In the EM method eddy current flow is induced in the ground by the time varying magnetic field of a vertical or horizontal magnetic dipole transmitter operating at a fixed frequency. The eddy current flow induces a secondary magnetic field which, together with the primary field, is sensed by a similar receiver dipole. The ratio of the primary and secondary fields is related to the conductivity of the subsurface.

The instrument parameters, frequency and coil separation, are selected so that operation can be described by the low induction number approximation. In this sense each induced eddy current loop is independent of the others and the measured (apparent) conductivity can be thought of as a linear superposition of the responses of strata within the exploration range of the array used.

Under certain restrictions concerning the maximum value of terrain conductivity the measured and strata conductivities are related by the following expression:

$$\sigma_a = \sum_{i=1}^n \sigma_i \cdot (R_i - R_{i-1}) \quad (8)$$

where σ_a is the apparent conductivity
 σ_i is the conductivity of the i th layer, and
 R_i, R_{i-1} are geometric (weighting) factors
characteristic of the top and bottom of the i th layer.

The effective exploration depth of the EM equipment can be varied by changing one or more of loop spacing (s), loop orientation (vertical or horizontal), or height above terrain (h_0). All these parameters affect the distribution of the geometric factors. For horizontal coplanar loops geometric factors are described by

$$R(D) = (D^2 + 1)^{-1/2} \quad (9)$$

and for vertical coplanar loops

$$R(D) = [(D^2 + 1)^{1/2} - D] \quad (10)$$

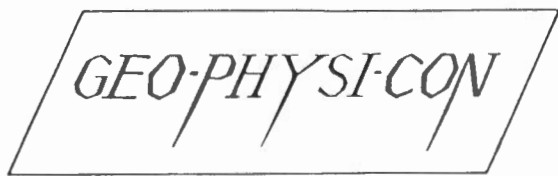
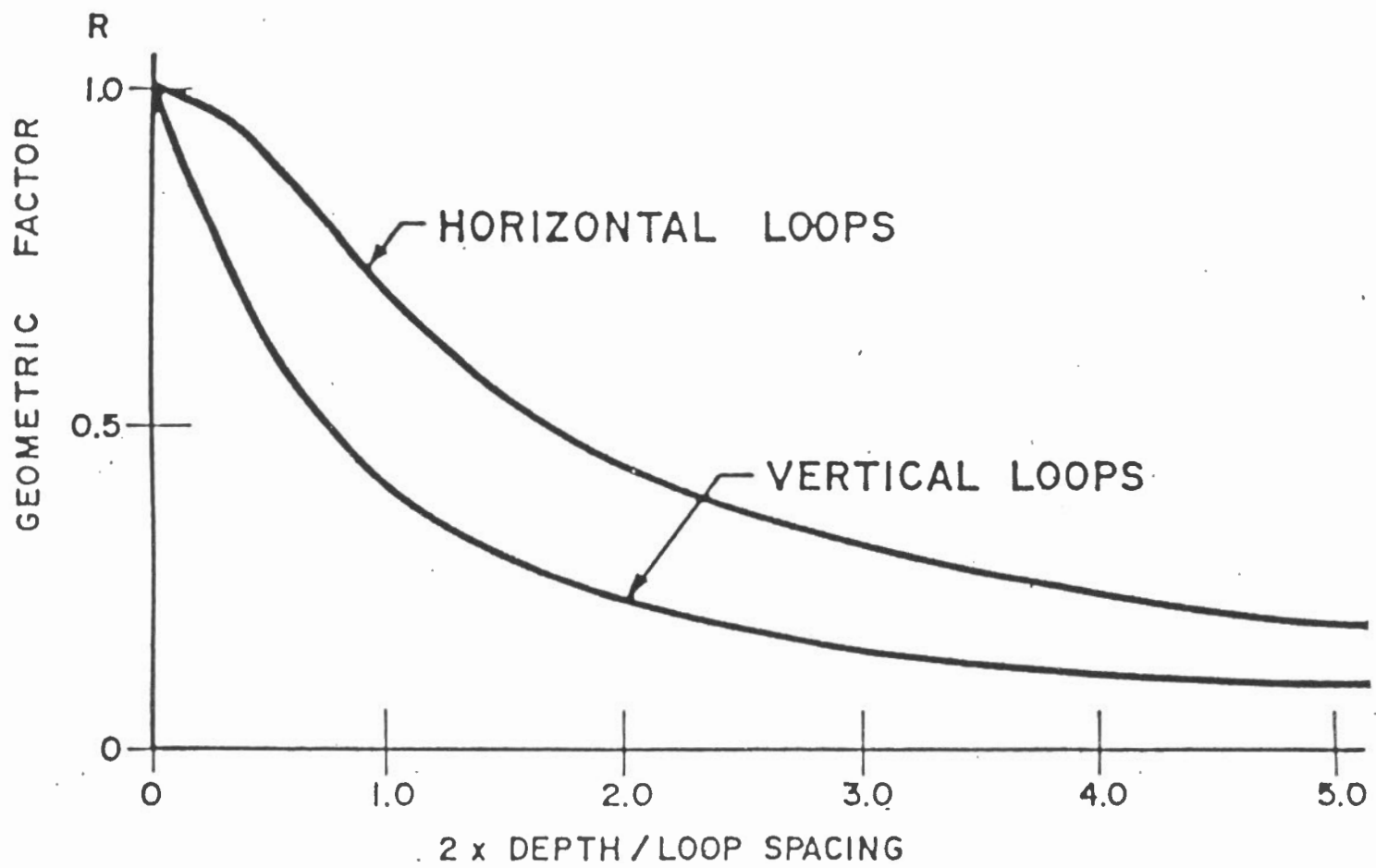
where the parameter $D = 2(h_0 + d)/s$ (11)

and d is the depth below ground surface

A graph of the functions (9) and (10), above, is shown in Figure 12. From this figure it is evident that, for a common loop spacing, the horizontal loop mode senses effectively twice as deep as the vertical loop mode. The units of apparent conductivity used in this work are millimhos/metre. For the TEM method the units for apparent resistivity are ohm-metres. These are related by

$$(\text{mmho/m}) = (\text{ohm-m})^{-1} \times 10^3$$

Detailed manufacturer's specifications for the instruments used are given in Appendix A.



ENGINEERING GEOPHYSICAL CONSULTANTS

GEOMETRIC FACTORS FOR
HORIZONTAL AND VERTICAL LOOPS

C 83-12

Figure 12

5.0 INTERPRETATION METHODS

5.1 General

Apparent resistivity curves have been prepared for data gathered using transmitter loop sizes of 100m by 100m and 400m by 400m for the late stage definition of apparent resistivity. The apparent resistivity curves obtained show the variety of geoelectric sections in accordance with the variations of resistivity distributions along the survey lines.

The fact that earth materials typically show larger resistivities when frozen than when unfrozen is well documented in the literature (2). The resistivity contrast between frozen and unfrozen sediments of the same type is the basis for the detection of permafrost using electrical methods.

The values of resistivity obtained from the interpretation created a basis for consideration of certain layers as frozen or unfrozen.

5.2 Relative and Absolute Coordinates

The interpretation of transient sounding data is mainly carried out by comparison of observed data to theoretical response of models. The theoretical response of the model can be expressed in either dimensionless parameters (relative coordinates - reference Figure 7) or in dimensioned parameters (absolute coordinates). The process of data interpretation at first determines as many parameters as possible for curve fitting using relative coordinate master curves. The reliability of the interpretation and identification of poorly defined parameters is then accomplished by comparison of the observed data and model response in absolute coordinates. In Section 6.0, the observed data and modelled response are shown superimposed using the late stage apparent resistivity definition at several stations for both loop sizes at both sites surveyed.

5.3 The Description of Apparent Resistivity Curves

All of the apparent resistivity curves obtained during this survey can be grouped depending upon the geoelectric sections to which they correspond, that is, in accordance with their shape.

5.3.1 Three layers, H-type Curves ($\rho_1 > \rho_2 < \rho_3$)

The curves of this type were obtained over Parsons Lake. Examples are presented in Figures 21 and 22 superimposed on the model curves. The characteristic features of the curves corresponding to both 100m x 100m and 400m x 400m transmitter loops are:

- i) left descending branch
- ii) minimum
- iii) right ascending branch

The left descending branches show the effect of a decrease of resistivity with depth. Their behaviors are characteristic for the resistivities of the first and second layers and the thickness of the first layer.

The minimum point is influenced mainly by the thickness and resistivity of the second layer.

The right ascending branch is used to determine the resistivity of the basement.

5.3.2 Three Layers, Q-type Curves ($\rho_1 > \rho_2 > \rho_3$)

The curves of this type were obtained over deeply frozen terrain. An example is given in Figure 17 being superimposed on the model curve.

The oscillations in the beginning of the curve are due to inductive phenomena, described elsewhere (1). Then, as time increases, apparent resistivity decreases continuously. Sometimes, depending on resistivities and thicknesses of the layers, deflections can appear.

5.3.3 Four Layers, HK-type Section ($\rho_1 > \rho_2 < \rho_3 > \rho_4$)

The curves of this type were obtained over most of the Big Lake site (Taglu field). They can represent both a completely frozen section and a section containing a talik. An example of the curve of this type superimposed on the model curve is given in Figure 16. The conclusion about the frozen or unfrozen state of sediments is made on the basis of absolute values of resistivity.

The characteristic features of the curves, corresponding to both transmitter loops sizes are:

- i) left descending branch
- ii) minimum point
- iii) ascending branch
- iv) maximum point with following right hand descending branch

The features i to iii show the same characteristics of geoelectric section as were described in 5.3.1. The maximum point and the following descending branch are characteristic for the thickness of the third layer and the resistivity of the basement.

5.3.4 Four Layers, QQ-type Curves ($\rho_1 > \rho_2 > \rho_3 > \rho_4$)

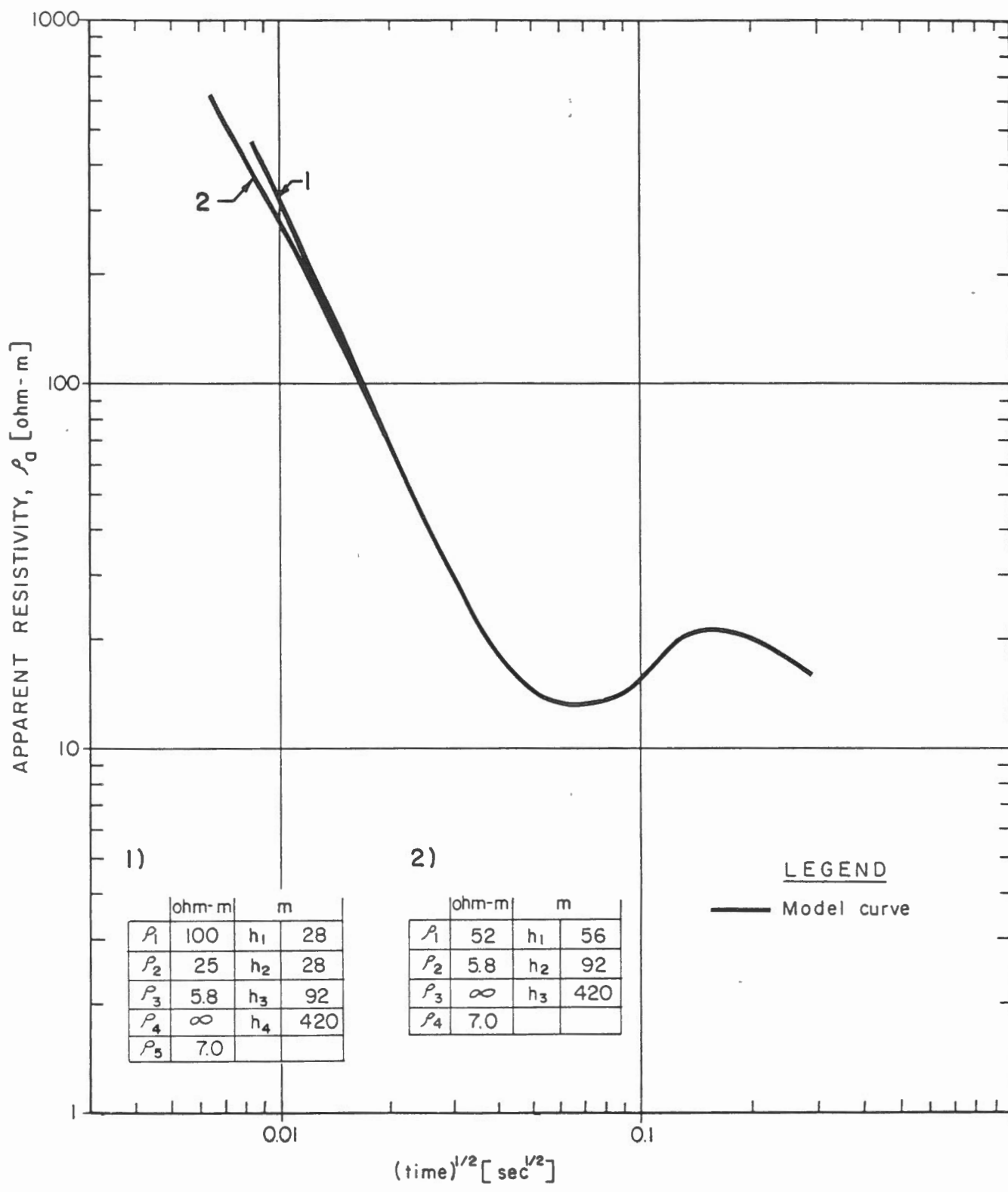
The curves of this type were obtained over the onland portion of the Parsons Lake site and at several stations of the Big Lake site. The examples are given on Figures 18 and 23. The curves show gradual decrease of apparent resistivities with time. Depending on resistivities and thicknesses of the individual layers, deflections can appear.

5.3.5 Multilayered Sections

Individual properties of the sections can bring additional geoelectric boundaries. For example, additional taliks encountered at Stations 2 and 3, Big Lake site, transforms the four layer sections, described in Section 5.3.3, into six layer sections.

It has been found by many investigators of permafrost that near surface permafrost has usually a complex geoelectric structure (2). Thin layering or a gradual change of resistivity with depth makes the recovering of actual distribution of resistivity very time consuming, if possible. At the same time, the layering within frozen intervals was assumed to be not of substantial interest. This creates a problem of replacing several thin layers by an equivalent layer of certain resistivity and thickness. These two parameters should be determined such that they create a minimal influence on the determination of the distribution of frozen and unfrozen ground.

Figure 13a shows the comparison of a five layer curve and a four layer curve with the first layer parameters equivalent to the first two layers of the five layer curve. It can be seen



1)

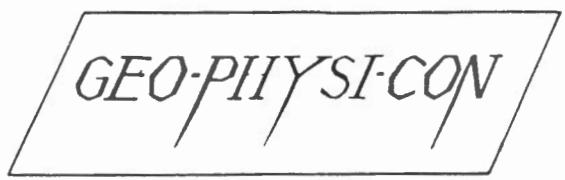
	ohm-m		m
ρ_1	100	h_1	28
ρ_2	25	h_2	28
ρ_3	5.8	h_3	92
ρ_4	∞	h_4	420
ρ_5	7.0		

2)

	ohm-m		m
ρ_1	52	h_1	56
ρ_2	5.8	h_2	92
ρ_3	∞	h_3	420
ρ_4	7.0		

LEGEND

— Model curve



REPLACEMENT OF
TWO LAYERS
BY ONE EQUIVALENT LAYER

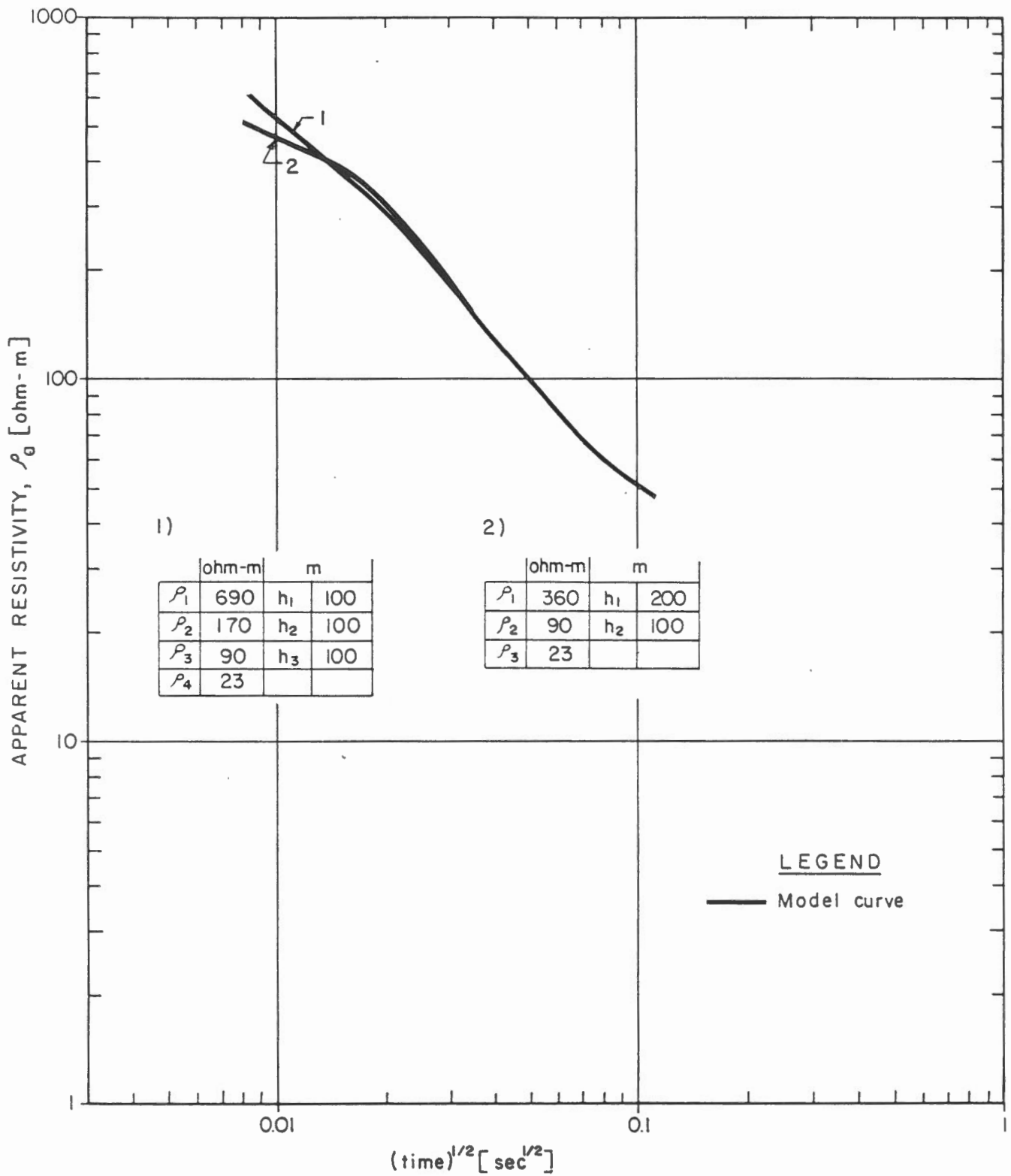
that the curves deviate in the beginning part and then merge. Thus, interpretation of the four layer curve will give the same values for the thicknesses of frozen and unfrozen layers.

The effect of the replacement of two layers by one equivalent layer for the section of QQ-type is given in Figure 13b. Again, the curves deviate at early time channels and then merge.

5.4 The Distortions of the Apparent Resistivity Curves

All of the theory and the technique of interpretation of TEM sounding data is based on the assumption that the section consists of a number of layers separated by boundaries which are parallel to the surface. In the present survey this was not always the case. The presence of lateral inhomogeneities distorts more or less the apparent resistivity curves obtained. The question arises to which loop size is subjected to stronger distortions.

There are two opposite effects. Lateral resolution can be expected to be better with the small loop size. Averaging ability is much stronger with the larger loop size, therefore, some distorting effects can be expected to interfere and to purge



GEO-PHYSI-CON

REPLACEMENT OF
TWO LAYERS
BY ONE EQUIVALENT LAYER

each other. The affects of distortions must be considered for each specific sounding.

5.5 Fixed Frequency EM Data

The fixed frequency data was gathered along both survey lines using six different measurement modes. The quantitative interpretation of the data was impossible because of the complexity of the resistivity distribution within the upper 50m and the absence of drill hole control. Due to these facts, fixed frequency profiles were used mainly qualitatively. The absolute values of the apparent conductivity were used to get better ideas about the resistivities of the upper parts of the sections in interpretation of TEM soundings.

6.0 RESULTS

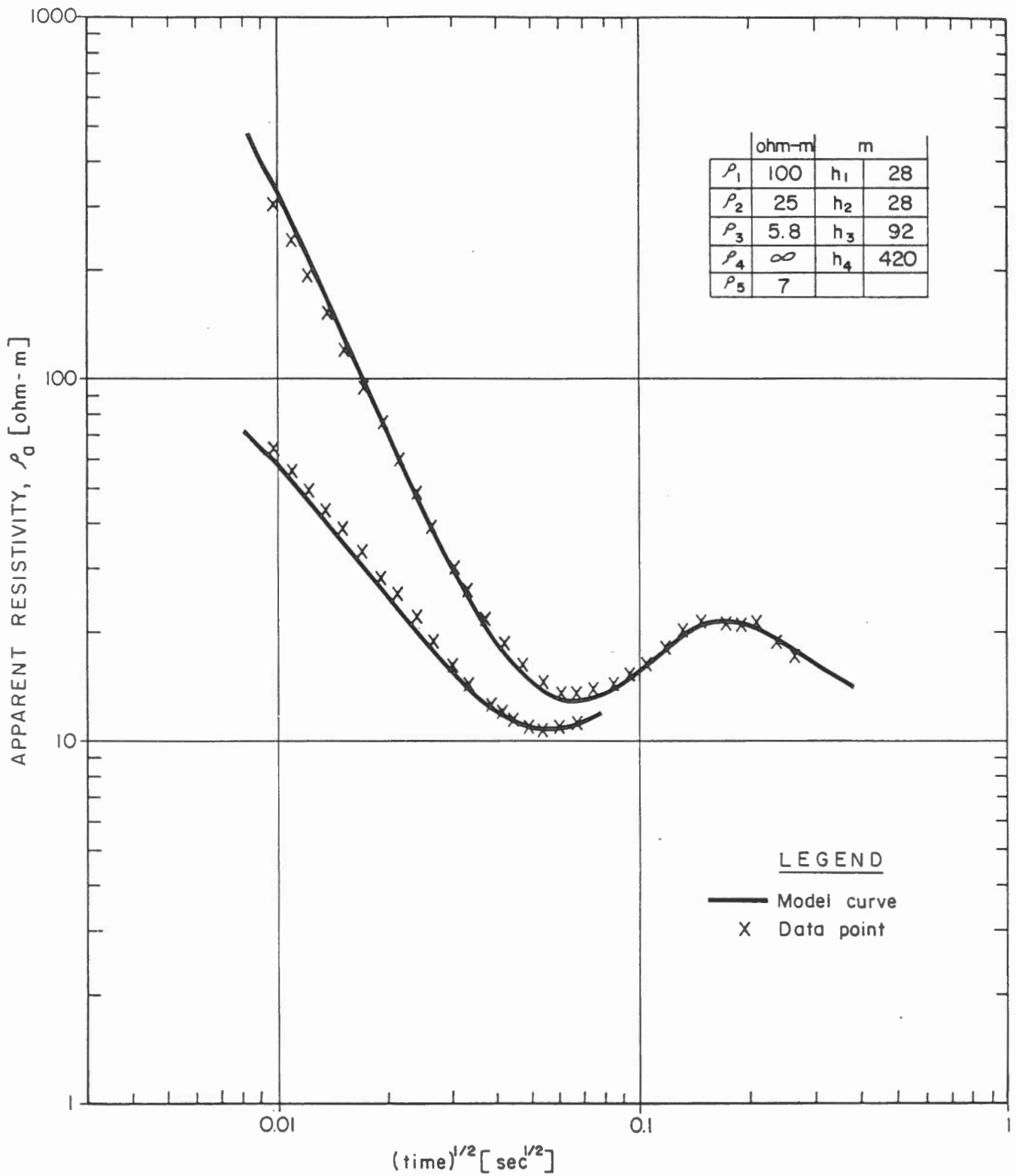
The results of the survey are presented for each site separately.

6.1 Taglu Site

Figure 14 gives the section derived from the interpretation of apparent resistivity curves. The examples of fitting the measured and model curves are given in Figures 15 to 18. The deviation of measured and model curves in the early time range is due to a more complex structure of permafrost than was used in modeling. These deviations have a negligible influence on the main interpreted parameters as discussed in Section 5.3.5.

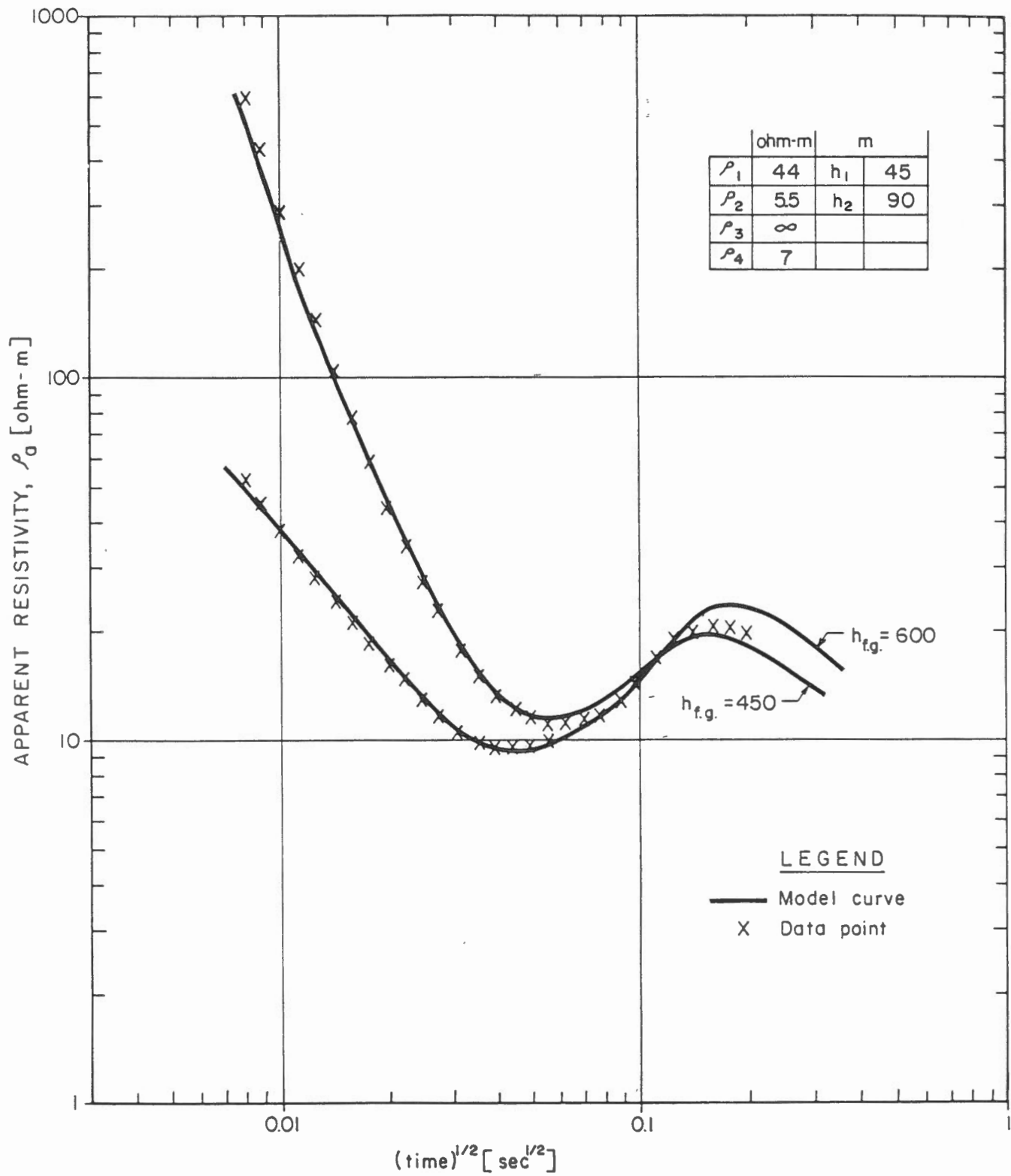
The fixed frequency profiles are given in Figure 19a, b, and c. The high apparent conductivity at Station 3+00 is due to a buried linear conductor (3). All of the other peaks correspond to the taliks and are described below.

In general, the section has a four-layer structure. Near surface frozen ground overlies a shallow unfrozen layer which, in turn, overlies a thick portion of frozen ground underlain by unfrozen material. Along the survey line this four layer section degrades to either three layers (when the first frozen layer is absent) or to two layers (when the section is frozen throughout).



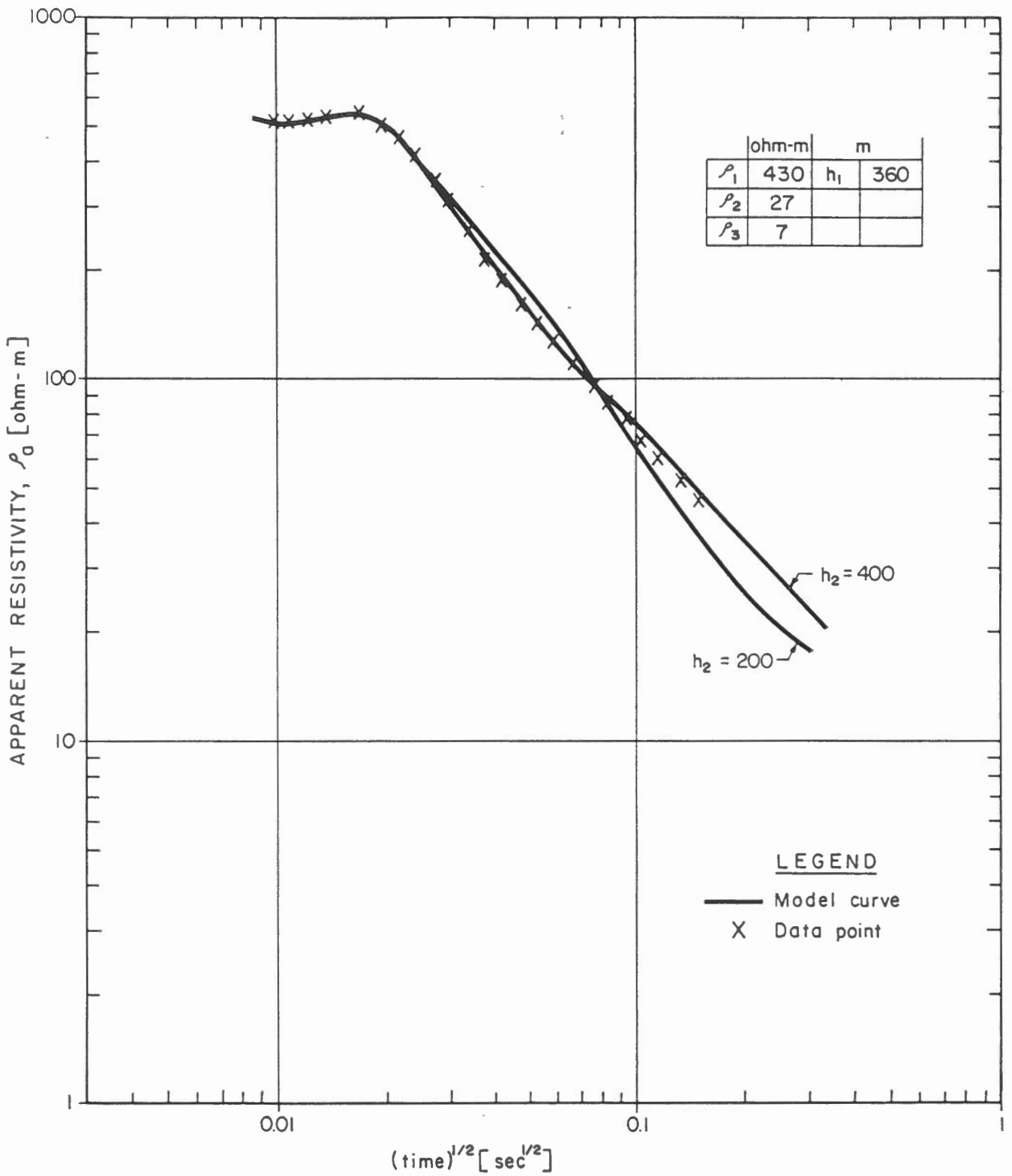
GEO-PHYSI-CON

TEM MEASURED AND
MODELLED CURVES
TAGLU FIELD
STATION I



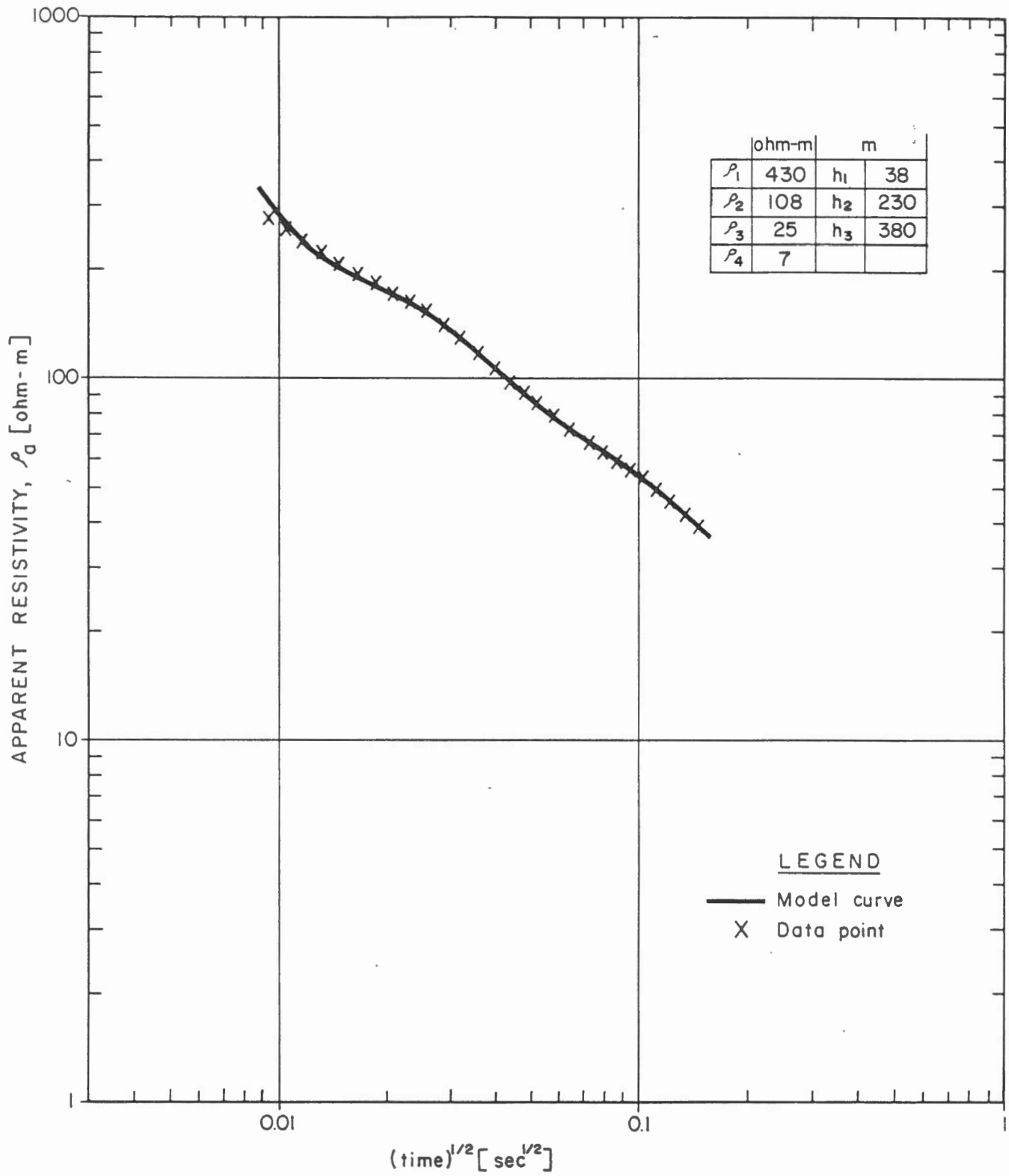
GEO-PHYSI-CON

TEM MEASURED AND
MODELLED CURVES
TAGLU FIELD
STATION 4



GEO-PHYSI-CON

TEM MEASURED AND
MODELLED CURVES
TAGLU FIELD
STATION 14



GEO-PHYSI-CON

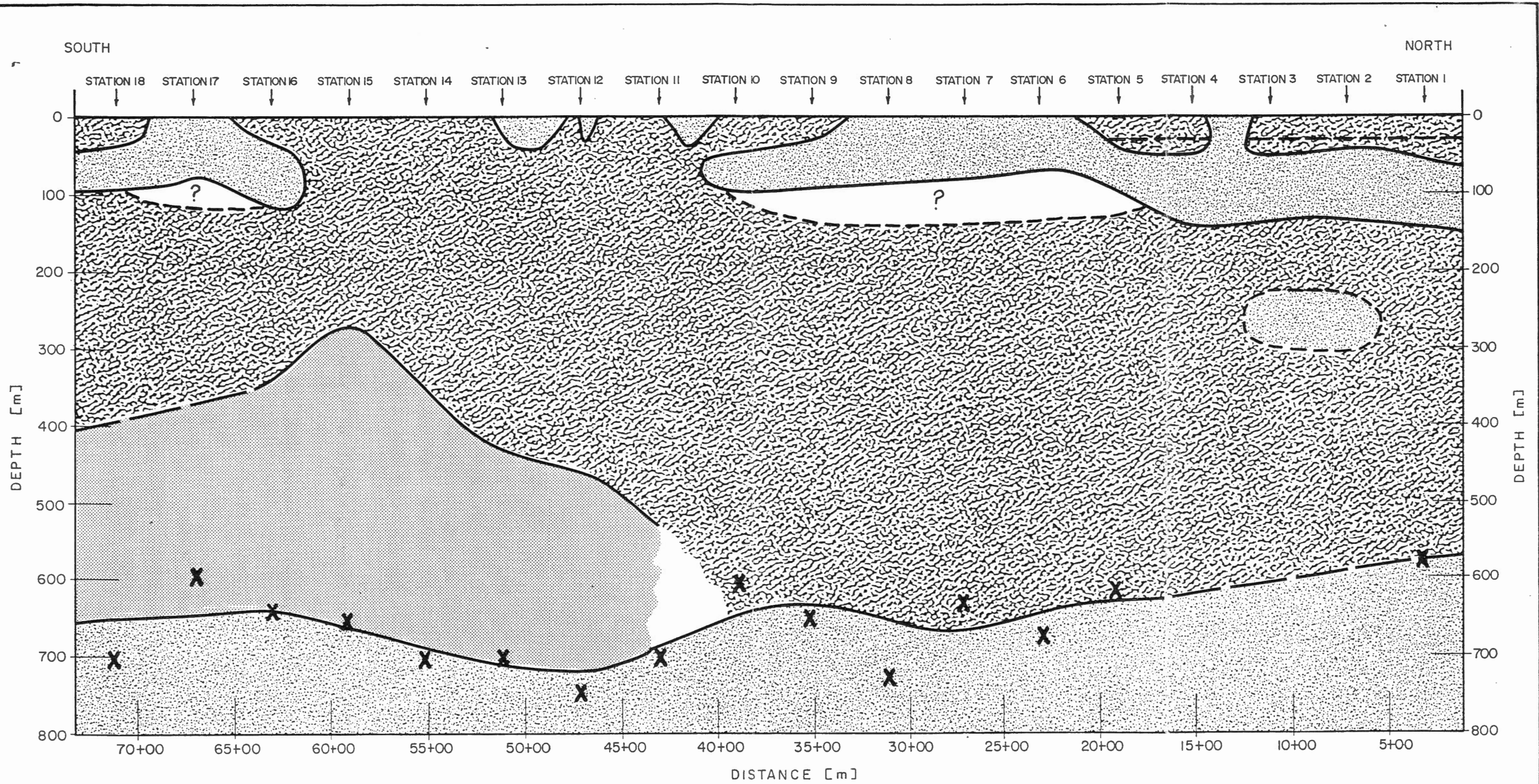
TEM MEASURED AND
MODELLED CURVES
TAGLU FIELD
STATION 15

ABSTRACT


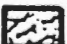

Electromagnetic soundings were carried out along on two lines in the Mackenzie Delta area to test the technique for ability to map the base of permafrost and to detect internal detail within the main body of the permafrost. A line in the north-east of Parson's Lake indicated permafrost thickness in good agreement with geothermal data but revealed that no permafrost exists beneath the lake itself. A second line across the Taglu area confirmed the relative constancy of the permafrost base across the area contrasted with the great complexity of shallow permafrost conditions. This area appears to be on onshore analogue of the offshore Beaufort Sea.

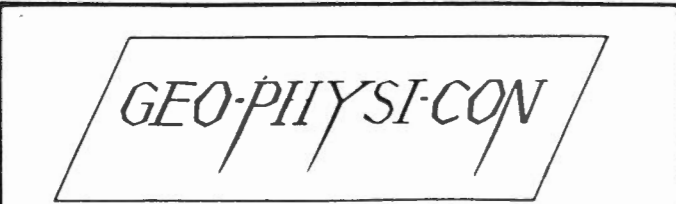
RESUME

Des sondages électromagnétiques ont été réalisés le long de deux traverses dans le Delta du Mackenzie pour évaluer la capacité de cette technique de tracer la base du pergélisol et de détailler son caractère interne. Une traverse dans la région du lac Parsons indique une épaisseur de pergélisol au nord-est du lac en bon accord avec les données géothermiques, mais ne révèle aucun pergélisol sous le lac. Une deuxième traverse corrobore la constance relative de la base du pergélisol dans la région de Taglu où, par opposition, le caractère du pergélisol superficiel est très complexe. Cette région semble représenter une analogie terrestre des conditions sous la mer Beaufort.

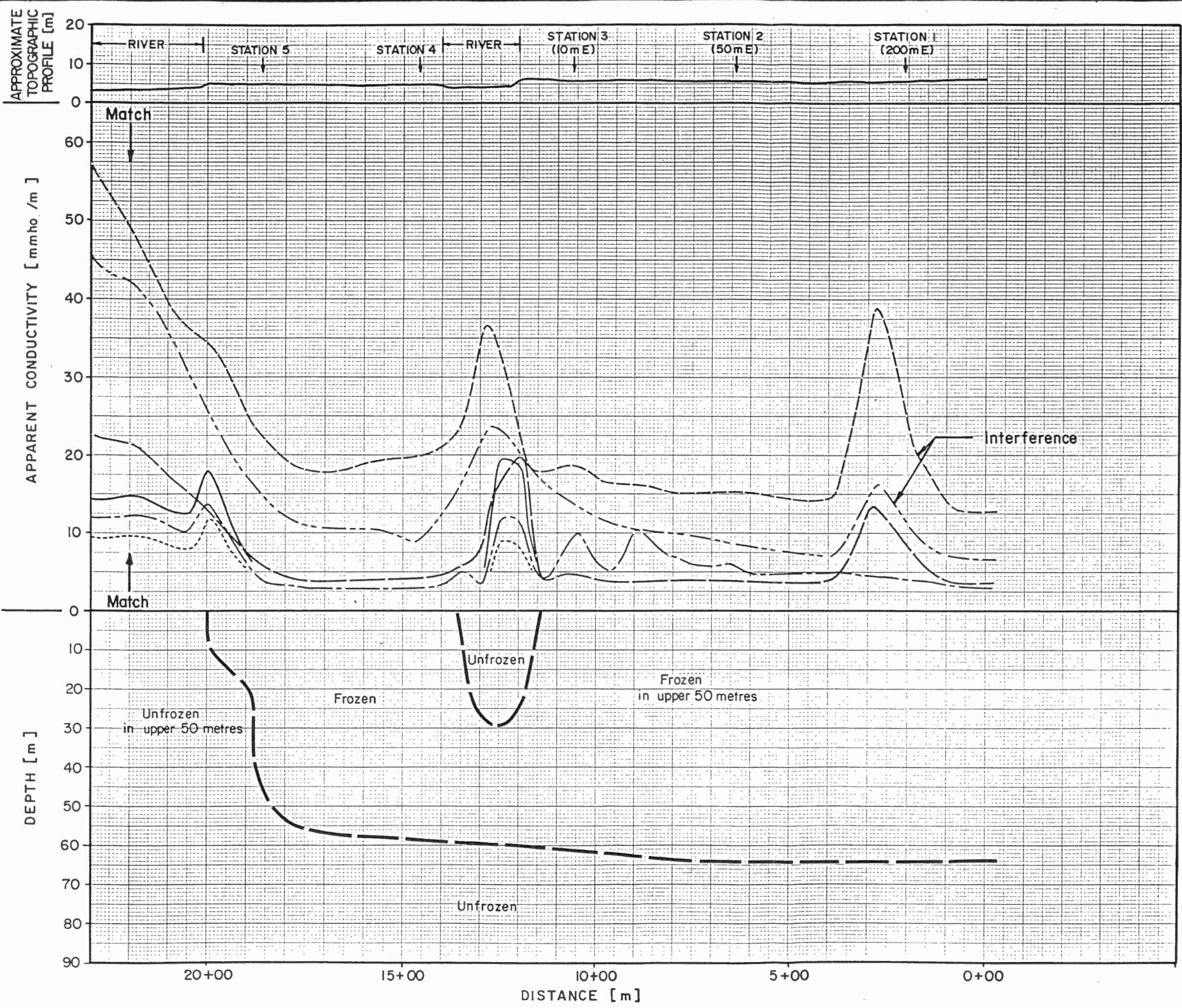


LEGEND

-  Unfrozen Ground
-  Frozen Ground
-  Frozen Clay (See Text)



EARTH PHYSICS BRANCH
 INTERPRETED SECTION
 BIG LAKE SITE
 TAGLU FIELD



LEGEND

- EM 34 (40 V)
- - - EM 34 (40 H)
- - - EM 34 (20V)
- EM 31 (HG)
- - - EM 31 (HZ)
- EM 31 (VG)

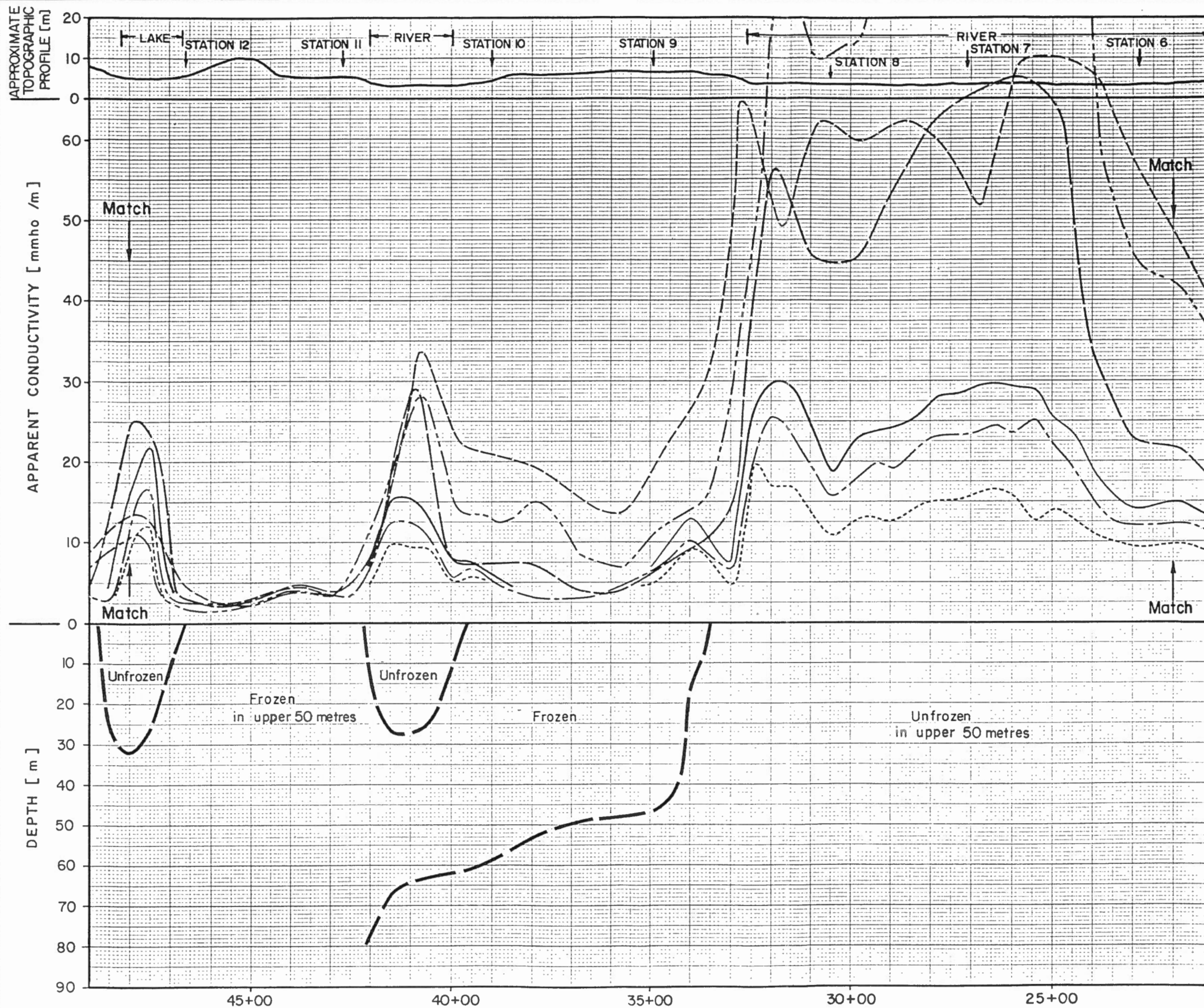
SCALE

Horizontal 1:10,000
 Vertical 1:1,000

NOTE: Depths shown are approximate only.

GEO-PHYSI-CON

FIXED FREQUENCY (EM) DATA
 TAGLU AREA
 E, M and R,
 EARTH PHYSICS BRANCH



LEGEND

- EM 34 (40 V)
- - - EM 34 (40 H)
- EM 34 (20V)
- EM 31 (HG)
- - - EM 31 (HZ)
- EM 31 (VG)

SCALE

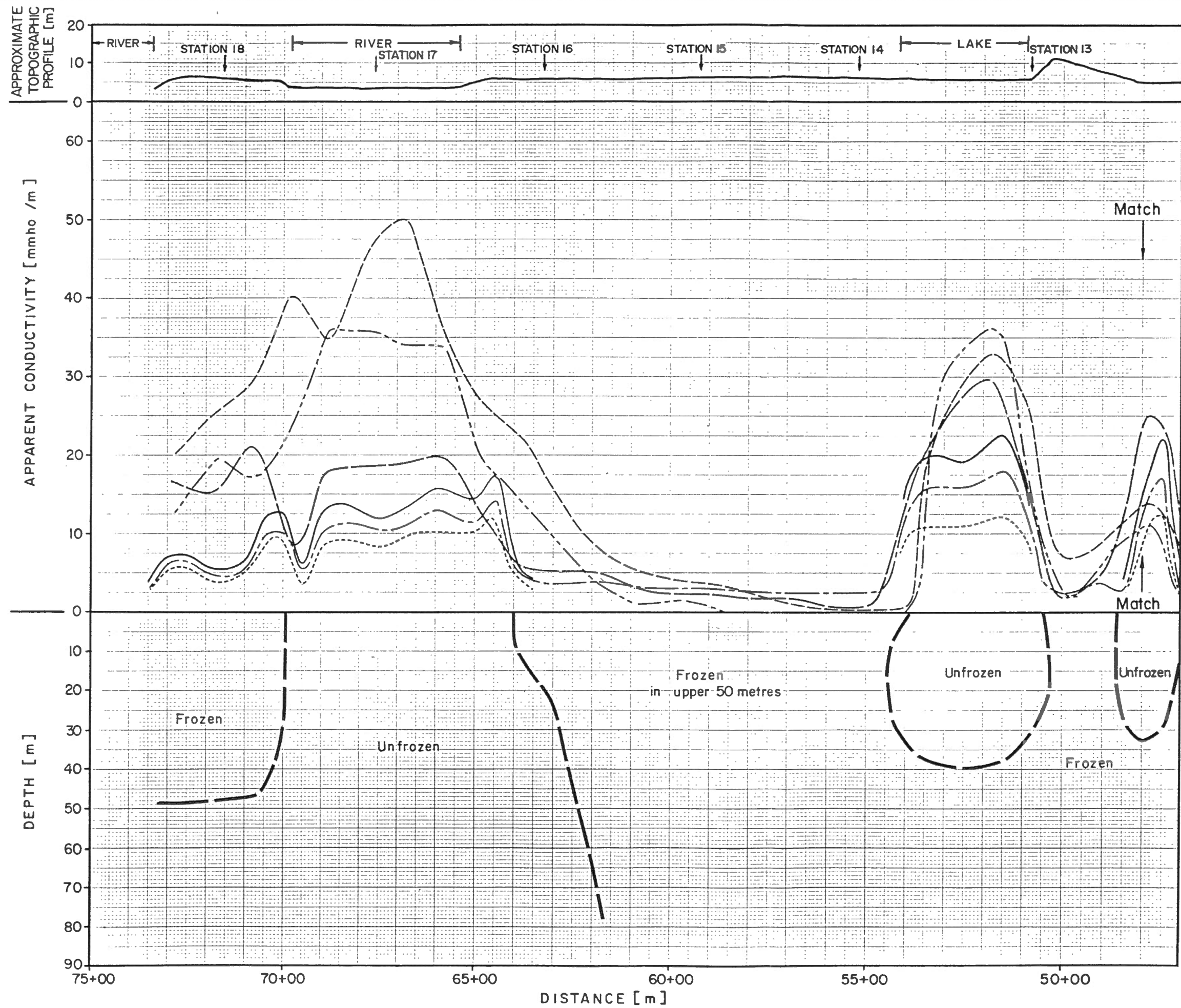
Horizontal 1 : 10,000
 Vertical 1 : 1,000

NOTE : Depths shown are approximate only.

GEO-PHYSI-CON

FIXED FREQUENCY (EM) DATA
 TAGLU AREA
 E, M and R,
 EARTH PHYSICS BRANCH

C 83-12 Figure 19b Cont'd



LEGEND

- EM 34 (40 V)
- - - EM 34 (40 H)
- EM 34 (20V)
- EM 31 (HG)
- - - EM 31 (HZ)
- · · EM 31 (VG)

SCALE

Horizontal 1 : 10,000
Vertical 1 : 1,000

NOTE : Depths shown are approximate only.

GEO-PHYSI-CON

**FIXED FREQUENCY (EM) DATA
TAGLU AREA
E, M and R,
EARTH PHYSICS BRANCH**

C 83-12 Figure 19c Cont'd

GEO-PHYSI-CON

A relatively thin layer of permafrost was found at the northern end of the survey line. This layer appears at the surface and has a thickness of up to 50m and an average resistivity of 40 to 50 ohm-m. More careful analysis allows recognition of additional boundaries within this layer. For example, at Station 1 a two layer structure with the first layer having a resistivity of 100 ohm-m and the second layer, a resistivity of 25 ohm-m can be expected. Slight deviations of the left branches shows that actually the upper frozen layer may have an even more complex structure.

The resistivity of 100 ohm-m unambiguously shows the frozen state of material in this environment. The resistivity of 25 ohm-m may correspond to either unfrozen silt (100 ohm-m when frozen) or frozen clay (5.5 ohm-m when unfrozen). Since the latter variant seems to be more probable, the whole layer is shown frozen on the section presented (Figure 14). Another possible position of the bottom of the first frozen layer is given by a dashed line at a level of about 25m between Stations 1 and 6.

A near surface talik shown in the section between Stations 3 and 4 corresponds to the current river channel. Its position was inferred from the fixed frequency data (Figure 19a).

The next layer has a resistivity of 4 to 6 ohm-m and represents unfrozen clay. Its bottom occurs at depths ranging from 100m to 150m between Stations 1 and 5.

The presence of the talik made it impossible to map the bottom of frozen material under the talik using the system employed. Due to this fact, the bottom of frozen ground was interpolated between Stations 1 and 4.

The surface frozen layer disappears between Stations 5 and 6 and further southward due to the warming influence of the river. The depth to the top of the resistive layer is reduced in this region. The top of the resistor occurs at a depth of about 75m (versus about 125m at Stations 1 to 4). It seems unlikely that the top of permafrost would become shallower beneath the river. This can be explained by the presence of a lens of sand under the river channel. Moderately resistive sand (e.g. 50 ohm-m) gives a resistivity ratio of 10 compared to the resistivity of the overlying clay (4 to 5 ohm-m). With the system used for this survey the boundary between the sandy lens and underlying frozen material is not mappable, and the top of permafrost is shown by the dashed line.

A four layer structure was encountered at Stations 9 and 10. The resistivity of the shallow conductive layer is equal to 12 to 15 ohm-m. Again this resistivity may be characteristic for either frozen clay with low ice content or unfrozen clayey silt. The more probable structure is given in the section presented in Figure 14.

The near surface taliks between Stations 10 and 11, at Station 12 and between Stations 12 and 13 are due to the intersection of the survey line with the river channel and two lakes, respectively. These near surface taliks were inferred using fixed frequency data.

Starting at Station 11 and further southward a layer with a resistivity of 25 to 40 ohm-m was encountered at depth. Its top is dipping northward and was traced to Station 16. It was impossible to trace it further northward from the existing apparent resistivity curves. The values of resistivity of 25 to 40 ohm-m can be characteristic for both frozen clay and unfrozen silt. To resolve this ambiguity additional information is required. Depending on which material is represented by this layer, the depth to the bottom of permafrost can vary substantially. It is more likely the layer represents frozen material.

Another surface talik is located between the Stations 16 and 18. Again, the structure similar to that at the Stations 9 and 10 can be seen. The values of resistivity for the near surface conductor at Stations 16, 17 and 18 are equal to 28, 6 and 5.5 ohm-m, respectively. The two latter values indicate unambiguously the unfrozen state of the material, while Station 16 shows the same ambiguity that was discussed above for Stations 9 and 10.

It should be pointed out that some apparent resistivity curves were distorted by lateral inhomogeneities. The curves obtained over completely frozen portions of the section (Station 11 to 15) are more likely distorted near the beginning (early time channels). The influence of the distortions on the determinations of the net depth of frozen ground is expected to be minimal. For the stations located in the vicinity of the river channel distortions take place at later time. The degree of their influence on the results of interpretation can only be estimated by comparison with drill hole data.

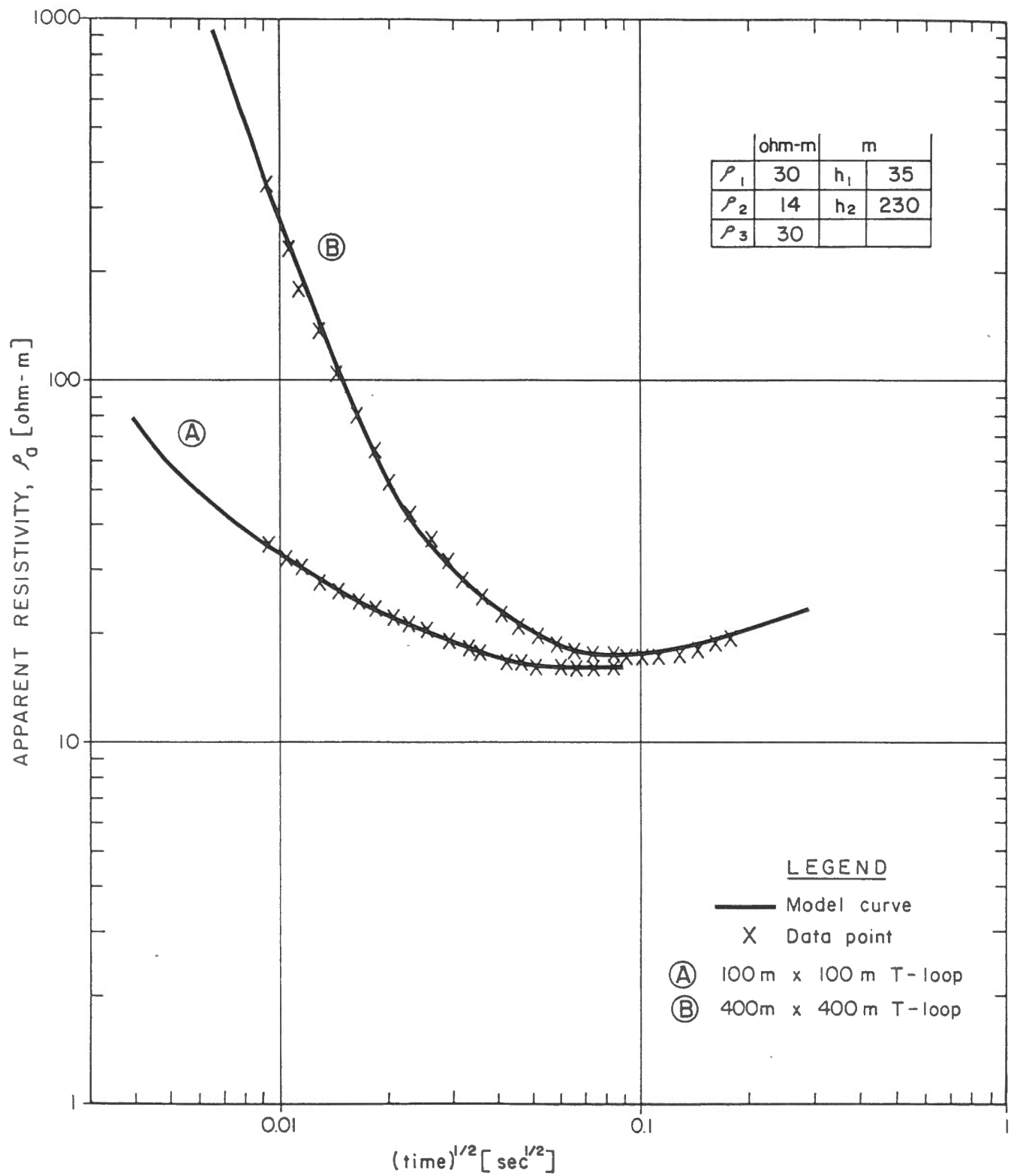
6.2 Parsons Lake

Figure 20 presents the section derived from the interpretation of apparent resistivity curves. The examples of fitting the measured and model curves are given in Figures 21 to 24.

The fixed frequency profiles are given in Figure 25. They show that the upper 50m of terrain south of Station 22+00 is of unfrozen material. North of this point the upper 50m of the section is totally frozen.

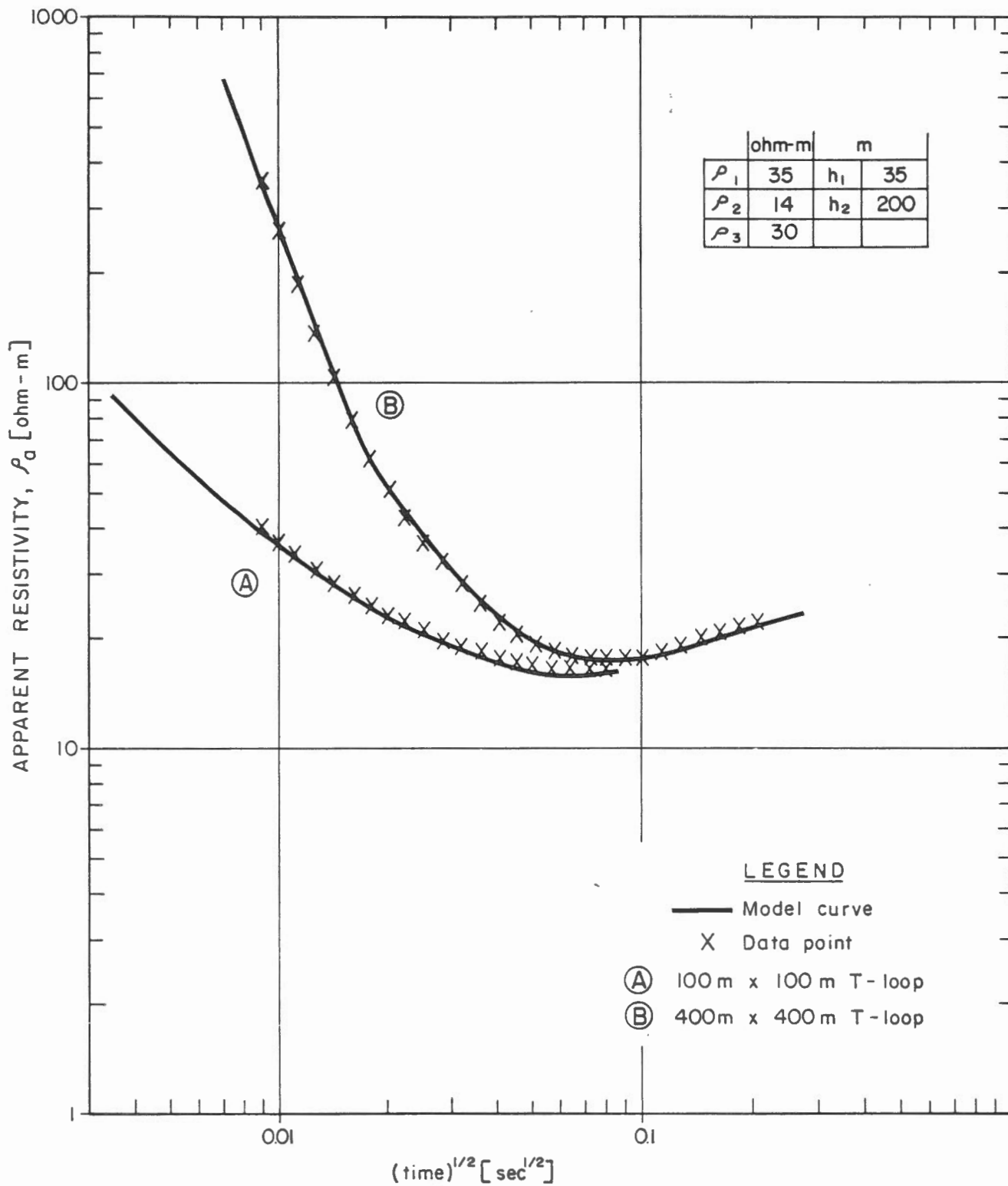
Two prominently different types of geoelectric sections were encountered along the survey line. In plan view they correspond to locations on Parsons Lake and to locations north of Parsons Lake.

Stations 1, 2 and 3 were measured on Parsons Lake. The interpretation of the curves obtained at Stations 1 and 2 indicates an unfrozen section. More careful analysis has shown that a thin layer of frozen ground (up to 50m) at a depth of 200m to 250m could be missed. However, it seems to be unlikely that a thin layer of frozen material would occur at this depth.



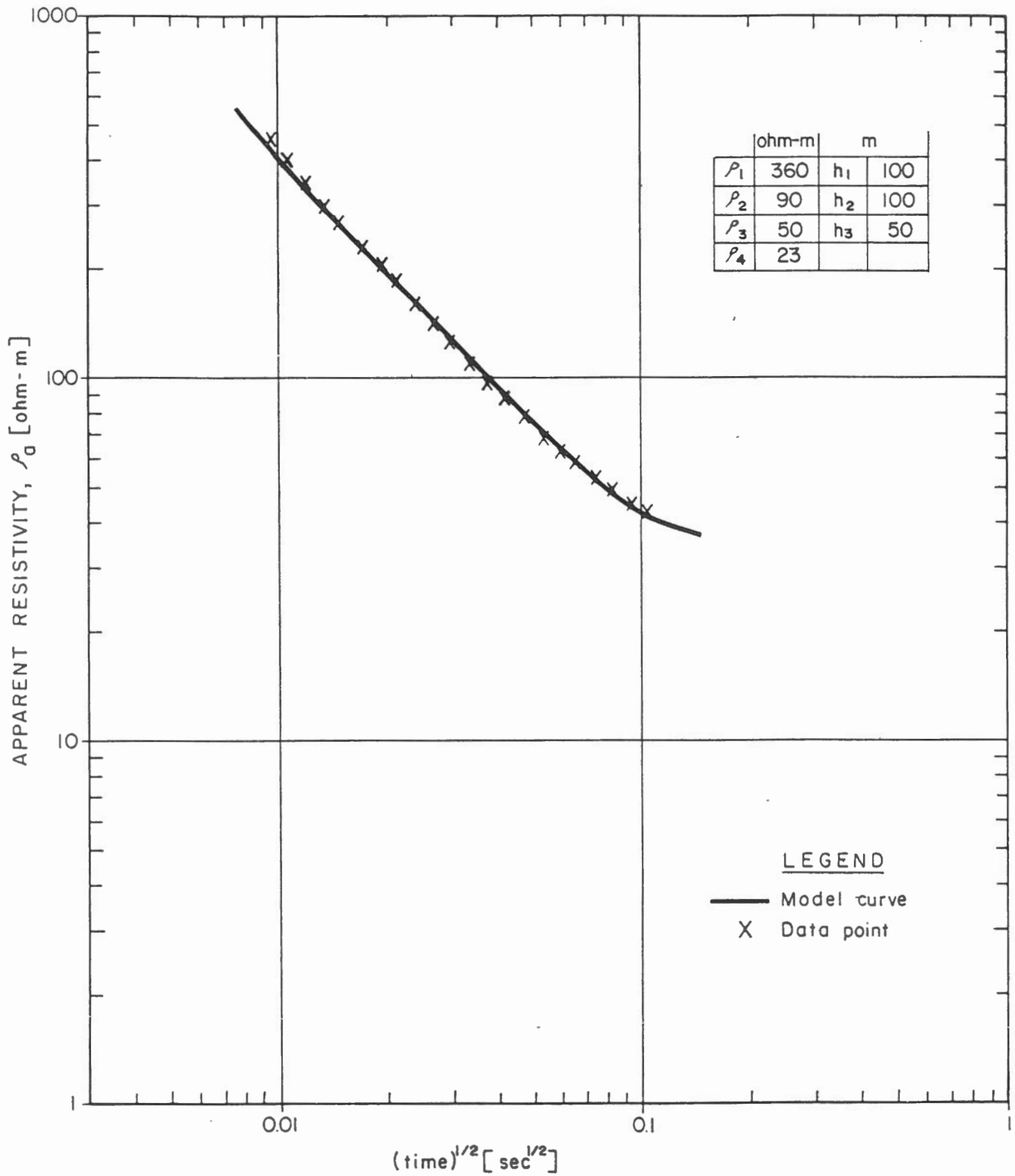
GEO-PHYSI-CON

TEM MEASURED AND
MODELLED CURVES
PARSONS LAKE
STATION I



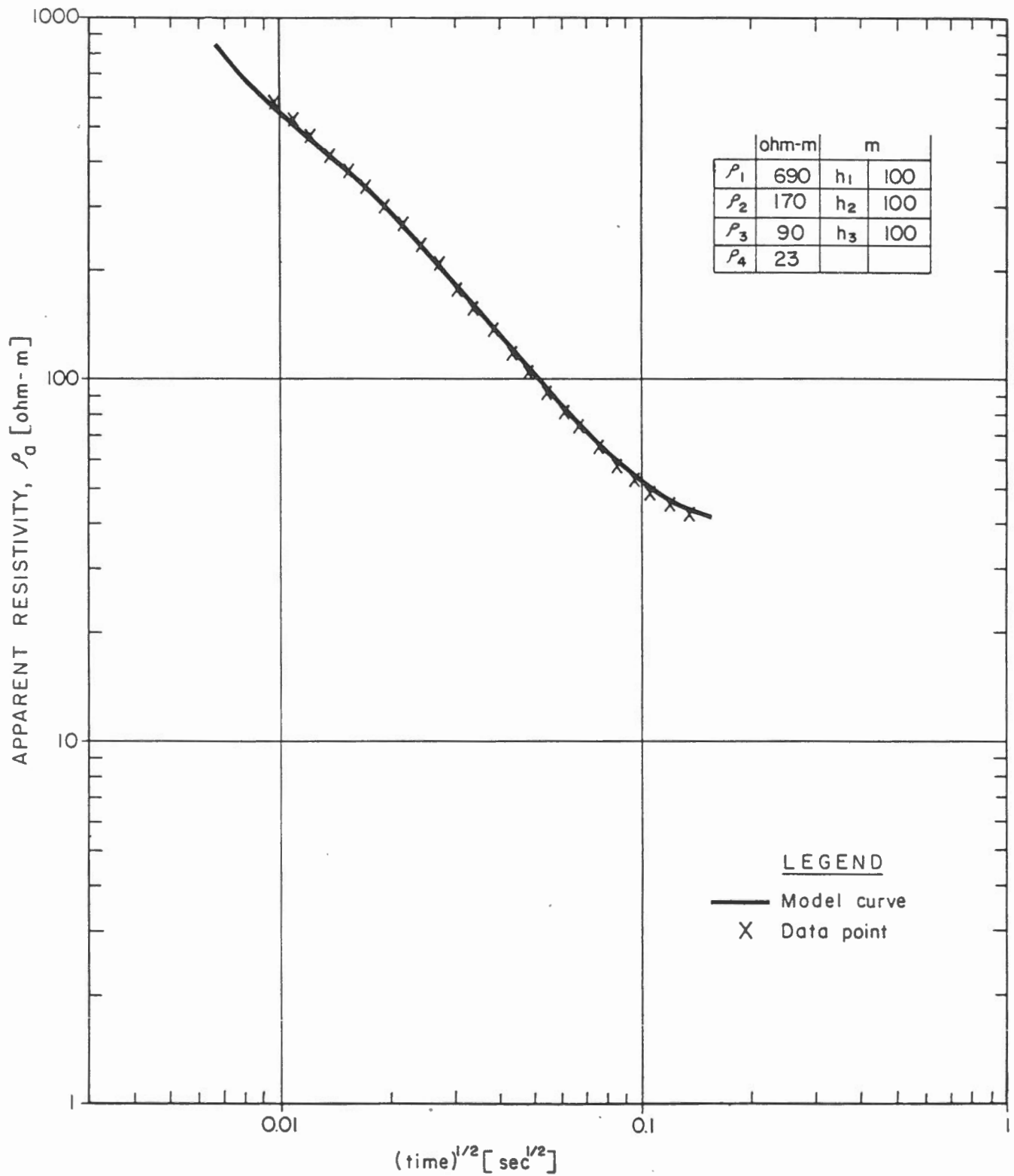
GEO-PHYSI-CON

TEM MEASURED AND
 MODELLED CURVES
 PARSONS LAKE
 STATION 2



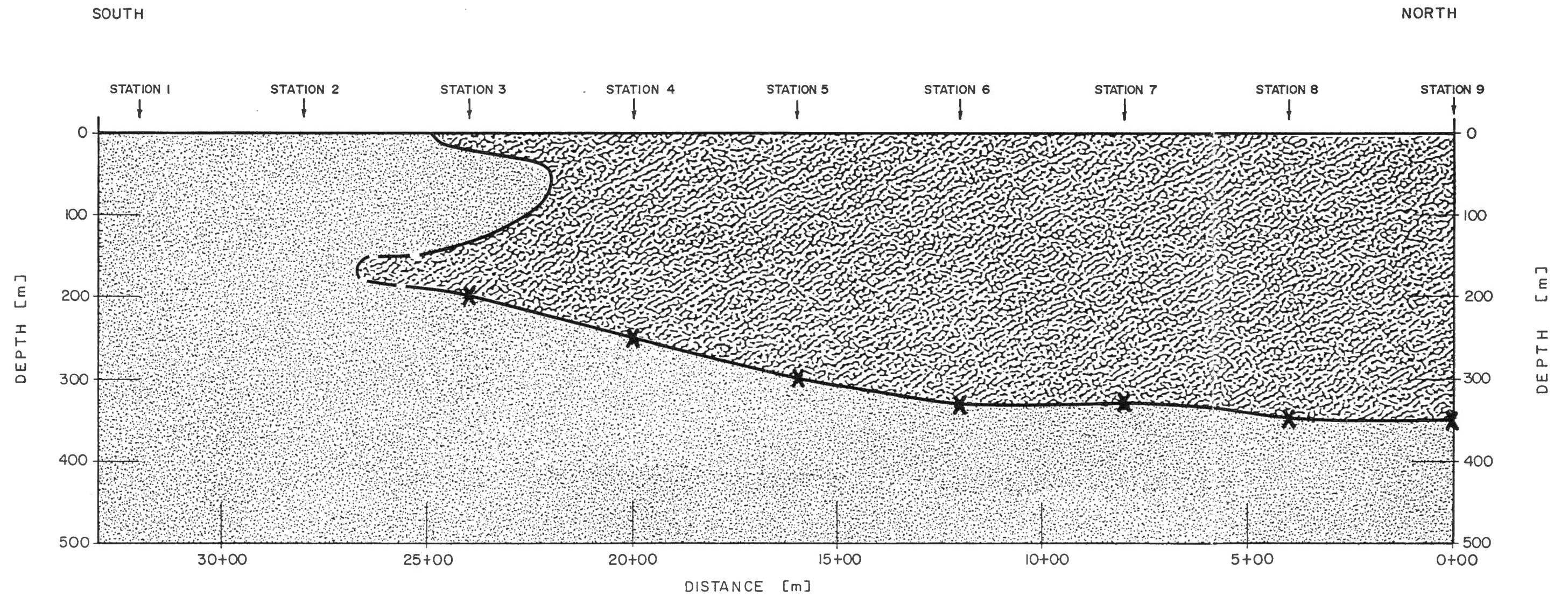
GEO-PHYSI-CON

TEM MEASURED AND
 MODELLED CURVES
 PARSONS LAKE
 STATION 4



GEO-PHYSI-CON

TEM MEASURED AND
 MODELLED CURVES
 PARSONS LAKE
 STATION 5

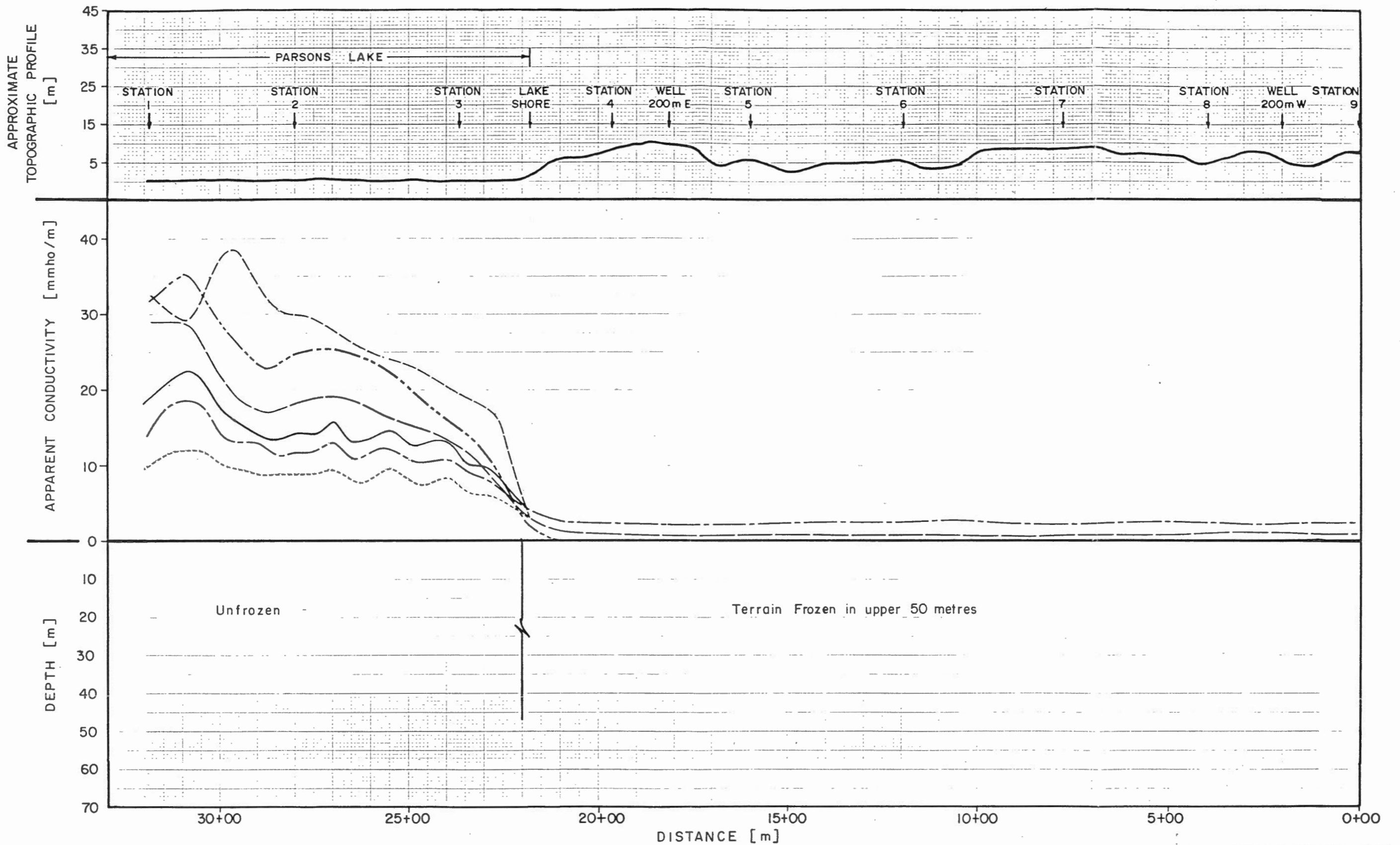


LEGEND

-  Unfrozen Ground
-  Frozen Ground

GEO-PHYSI-CON

EARTH PHYSICS BRANCH
 INTERPRETED SECTION
 BIG LAKE SITE
 PARSONS LAKE

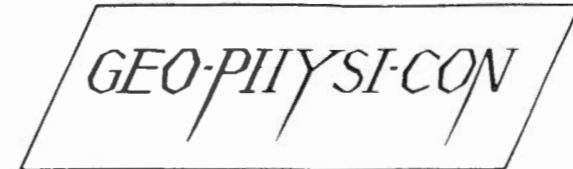


LEGEND

- | | |
|--------------------|------------------|
| ----- EM 34 (40 V) | ----- EM 31 (HG) |
| ----- EM 34 (40 H) | ----- EM 31 (HZ) |
| ----- EM 34 (20 V) | ----- EM 31 (VG) |

SCALE

Horizontal 1:10,000
Vertical 1:1,000



FIXED FREQUENCY (EM) DATA
PARSONS LAKE
E,M and R, EARTH PHYSICS BRANCH

The interpretation of the apparent resistivity curves from Stations 4 to 10 shows the section frozen from the surface. The depth to the bottom of permafrost increases slightly to the north. The depth to the bottom changes from 250m at Station 4 to 350m at Station 9.

Station 3 corresponds to the transition zone from the lake section to the onland section. The fixed frequency data shows a presence of the frozen "tongue" near the surface. The apparent resistivity curve indicates the presence of a frozen wedge at a depth of about 150m.

7.0 CONCLUSIONS AND RECOMMENDATIONS

It can be concluded from the results of the survey that the transient electromagnetic soundings were successful in the investigation of permafrost distribution, both in plan and in section view. The accuracy of the interpretation largely depends on the complexity of the geoelectric sections encountered and on the availability of additional information.

At the Big Lake site (Taglu Lake) the following features were detected:

- 1) Frozen ground has generally a two layer structure at the northern end of the survey area. Occasional unfrozen lenses can be present in the lower (thicker) frozen layer.
- 2) The first frozen layer is absent beneath the present river channel. Migrations of the channel can be inferred from the interpreted permafrost distribution.
- 3) In the hilly terrain the section is frozen throughout.
- 4) Two permafrost layers were encountered again at the southern end of the survey area.
- 5) A layer of frozen clay or shale is expected under the southern half of the survey line. This change in material type as compared to the material expected in the northern half, may correlate to the historical development of the Mackenzie Delta.

- 6) In general, the depth to the bottom of permafrost is expected to vary from 550m to 700m.

At the Parsons Lake site the section was found to be most likely unfrozen under Parsons Lake and frozen beneath the surrounding low hills. The depth to the bottom of permafrost is expected to vary from 250m to 350m.

Employment of two transmitter loop sizes has proven to be very useful. The data obtained with a loop of smaller size was used both for more constant interpretation and for the analysis of lateral distortions.

Fixed frequency EM survey turned out to be very beneficial. This inexpensive method gives valuable information about the lateral continuity of material and useful to the interpretation of TEM soundings.

In the interest of planning of future surveys a number of recommendations can be made. These deal with logistical support, survey technique and instrument modification.

- i) For the present survey, transportation to and from the survey site was accomplished using helicopters. A lengthy amount of time was required to move equipment between survey sites as four loads for equipment and one for the crew were required. About 1.5 to 2 hours of daily survey time were also lost due to daily transportation of the crew to and from Tuktoyaktuk. Additionally, there was a large potential to lose time in the event of equipment or snowmobile failure.

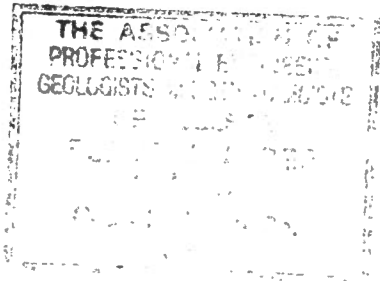
It is suggested for future surveys that the crew house in cat trains close to the survey sites. Less time would be lost to travel and adequate repair facilities would be closer at hand. Helicopters may still be required for movement of the equipment between sites a large distance apart.

- ii) For the present survey the vertical field of the transient electromagnetic response was measured. This field is, in general, proportional to conductivity to the power 1.5. Research has been underway over the last year to determine the usefulness of radial field data. The radial field is known to be proportional to the conductivity to a power of 2 and, therefore, contains more detailed information on the geoelectric section. The radial field data would be measured

GEO-PHYSI-CON

outside of the transmitter loop and would compliment vertical field data. The radial field has not been used for this purpose in the past and, and procedures for its use must be developed.

- iii) A weak signal strength limited the exploration depth under the specific geoelectric conditions. This can be remedied by transmitting greater current. A suitable generator is presently being sought.



Respectfully submitted,
GEO-PHYSI-CON CO. LTD.,

Per: Gr. Rozenberg

Grigory Rozenberg, M.Sc.
Senior Geophysicist

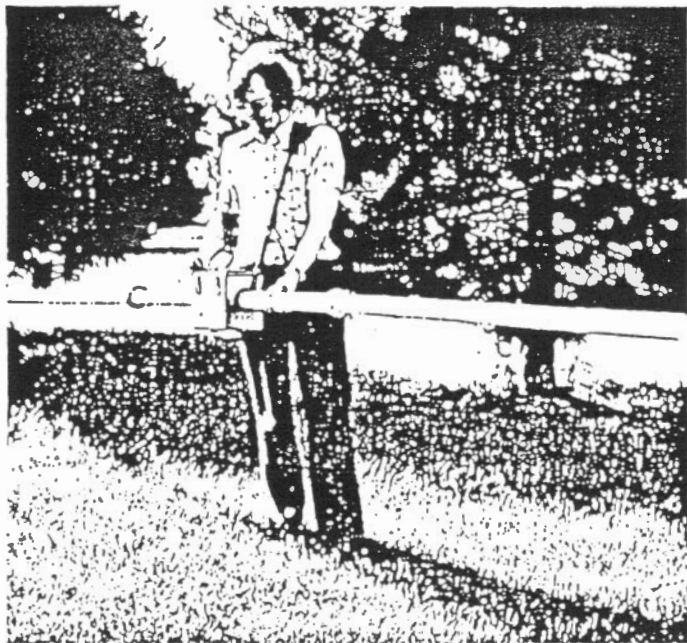
Per: T. Sartorelli

T. Sartorelli, P.Eng.,
Senior Geophysicist

Calgary, Alberta
June 1983
C83-12

References

1. Kaufman, A. A., and Morozova, G. M. 1970. The theoretical basis of transient sounding in the near zone. Nauka, Siberian Division, Acad. Sci. U.S.S.R.
2. Hoekstra, P. and D. McNeill. Electromagnetic probing of permafrost. Proc. Second Int. Conf. on Permafrost, Yakutsh, U.S.S.R., North Am. Contrib. NAS-NAC, 479, 1973.
3. Geonics Limited. Operating Manual for EM31 non-contacting terrain conductivity meter, 1979.



EM31

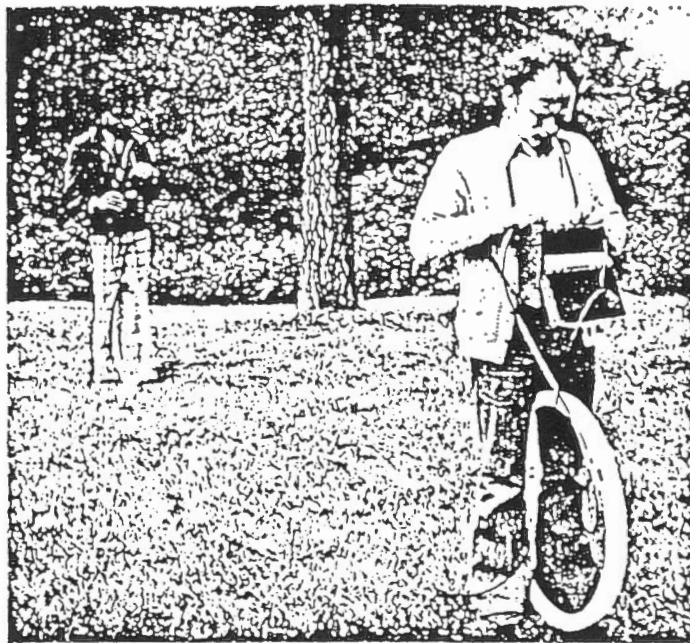
The Geonics EM31 provides a measurement of terrain conductivity without contacting the ground using a patented inductive electromagnetic technique. The instrument is direct reading in millimhos per meter and surveys are carried out simply by traversing the ground.

The effective depth of exploration is approximately six meters making it ideal for engineering geophysics. By eliminating ground contact, measurements are easily carried out in regions of high resistivity such as gravel, permafrost and bedrock. Over a uniform half space the EM31 reads identically with conventional resistivity and the measurement is analogous to a conventional galvanic resistivity survey with a fixed array spacing. Interpretation curves supplied with each instrument often permit an estimate of a layered earth.

The advantages of the EM31 are the speed with which surveys can be carried out, the ability to precisely measure small changes in conductivity, and the continuous readout which provides a previously unobtainable lateral resolution.

Specifications

MEASURED QUANTITY	Apparent conductivity of the ground in millimhos per meter.
PRIMARY FIELD SOURCE	Self-contained dipole transmitter
SENSOR	Self-contained dipole receiver
INTERCOIL SPACING	3.66 meters
OPERATING FREQUENCY	9.8 kHz
POWER SUPPLY	8 disposable alkaline 'C' cells (approx. 20 hrs life continuous use)
CONDUCTIVITY RANGES	3, 10, 30, 100, 300, 1000 mmhos/meter
MEASUREMENT PRECISION	±2% of full scale
MEASUREMENT ACCURACY	±5% at 20 millimhos per meter
NOISE LEVEL	<0.1 millimhos per meter
OPERATOR CONTROLS	<ul style="list-style-type: none"> ● Mode Switch ● Conductivity Range Switch ● Phasing Potentiometer ● Coarse Inphase Compensation ● Fine Inphase Compensation
DIMENSIONS	Boom : 4.0 meters extended 1.4 meters stored Console : 24 x 20 x 18 cm Shipping Crate : 155 x 42 x 28 cm
WEIGHT	Instrument Weight : 9 kgm Shipping Weight : 23 kgm



EM34-3

Operating on the same principles as the EM31, the EM34-3 is designed to achieve a substantially increased depth of exploration and a readily available vertical conductivity profile.

The underlying principle of operation of this patented non-contacting method of measuring terrain conductivity is that the depth of penetration is independent of terrain conductivity and is determined solely by the instrument geometry i.e. the intercoil spacing and coil orientation. The EM34-3 can be used at three fixed spacings of 10, 20, or 40 meters and in the vertical coplanar (as shown) or horizontal coplanar mode. In the vertical coplanar mode, the instrument senses to approx. 0.75 of the intercoil spacing. In the horizontal coplanar mode, the instrument can sense to 1.5 times the intercoil spacing. For the horizontal coplanar mode, however, coil misalignment errors are more serious than in the vertical mode so greater care must be exercised to achieve the maximum 60 meter depth.

Simple operation, survey speed and straight forward data interpretation makes the EM34-3 a versatile and cost effective tool for the engineering geophysicist.

Specifications

MEASURED QUANTITY	Apparent conductivity of the ground in millimhos per meter
PRIMARY FIELD SOURCE	Self-contained dipole transmitter
SENSOR	Self-contained dipole receiver
REFERENCE CABLE	Lightweight, 2 wire shielded cable
INTERCOIL SPACING & OPERATING FREQUENCY	<ul style="list-style-type: none"> ● 10 meters at 6.4 kHz ● 20 meters at 1.6 kHz ● 40 meters at 0.4 kHz
POWER SUPPLY	Transmitter : 8 disposable 'D' cells Receiver : 8 disposable 'C' cells
CONDUCTIVITY RANGES	3, 10, 30, 100, 300 mmhos/meter
MEASUREMENT PRECISION	±2% of full scale deflection
MEASUREMENT ACCURACY	±5% at 20 millimhos per meter
NOISE LEVEL	< 0.2 millimhos per meter
DIMENSIONS	Receiver Console : 19.5 x 13.5 x 26cm Transmitter Console : 15 x 8 x 26cm Coils : 63cm diameter
WEIGHTS	Receiver Console : 3.1 kg Receiver Coil : 3.2 kg Transmitter Console : 3.0 kg Transmitter Coil : 6.0 kg Shipping Weight : 41. kg

EM37 Ground Transient Electromagnetic System
Technical Specifications

Transmitter

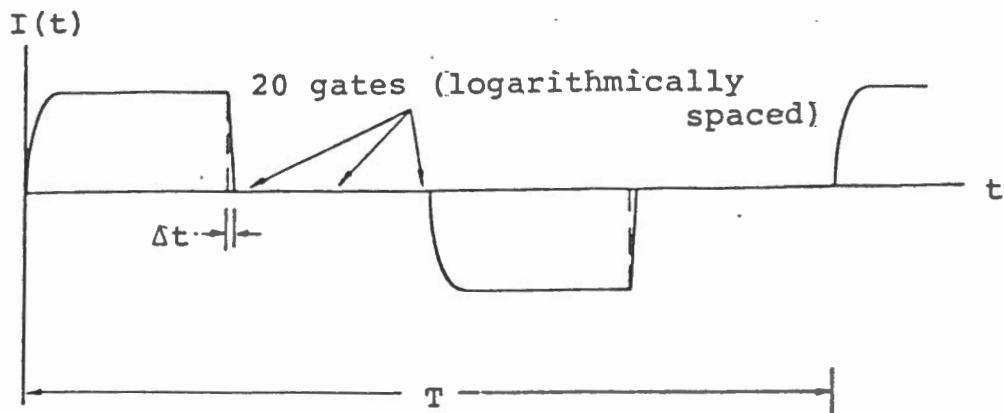
- Current Waveform - See Fig.A1
- Repetition rate - 3Hz or 30Hz in countries using 60Hz power line frequency; 2.5Hz or 25Hz in countries using 50Hz power line frequency; all four base frequencies are switch selectable.
- Turn-off time (Δt) - fast linear turn-off of maximum 300 μ sec. at 20 amps into 300x600m loop. Decreases proportionally with current and (loop area)^{1/2} to minimum of 20 μ sec. Actual value of Δt read on front panel meter.
- Transmitter loop - any dimensions from 40x40m to 300x600m maximum at 20 amps. Larger dimensions at reduced current. Transmitter output voltage switch adjustable for smaller loops. Value of loop resistance read from front panel meter; resistance must be greater than 1 ohm on lowest voltage setting to prevent overload.
- Transmitter protection - circuit breaker protection against input over-voltage; instantaneous solid state protection against output short circuit; automatically reset on removal of short circuit. Input voltage, output voltage and current indicated on front panel meter.
- Transmitter output voltage - 150 volts (zero to peak) maximum; 20 volts (zero to peak) minimum
- Transmitter output power - 2.8 kw maximum
- Transmitter wire supplied - 1800m. #10 copper wire PVC insulated with nylon jacket; transmitter wire contained on 6 reels (supplied); 2 reel winders supplied.
- Transmitter motor generator - 5 HP Honda gasoline engine coupled to 120 volt, 3 phase, 400Hz alternator. Approximately 8 hours continuous operation from full (built-in) fuel tank.

Receiver

- Measured quantity - time rate of decay of magnetic flux along 3 axes.
- Sensors - two air cored coils of bandwidths 11 and 50 kHz respectively; each 66cm dia.x4x5cm cross-section. Low frequency coil for general use, high frequency coil for shallow sounding.
- Time channels - 20 time channels with locations and widths as shown in Fig.A2. Successive operation at 30Hz, then 3Hz, effectively gives 30 channels covering range from 80 μ sec. to 80 msec.
- Output display - 4 figure digital LED plus sign; display also shows channel number and gain.
- Integration time - 2^n cycles at 30Hz; n=4,6,8,10,12,14 (switch selectable); similar integration times at other base frequencies.
- Receiver noise - approximately 1.5×10^{-10} volt/m²/turn of receiver coil at last gate at 30Hz with integration time of 34 seconds. Noise will be higher during intense local spherics activity.
- Output connector - all 20 channels available in analogue format from output connector at 5 volts fsd level.
- Synchronization to Tx - any of the following (switch selectable)
(1) reference cable
(2) primary pulse
(3) 27 MHz radio link (40 channels)
(4) high stability (oven controlled) quartz crystals.
- Noise rejection circuitry - with any of (1)-(3) above, entire system is automatically synchronized to 50/60Hz power line frequency when such interference exists in survey area; selective clipping of atmospheric noise pulses at all times. Audio output of Rx coil (transmitter pulse blanked out) is available on built-in loud speaker for ready identification of interference.
- Receiver batteries - 12 volt rechargeable Gel-cells; either 9 hours continuous operating time at 17°C (battery weight

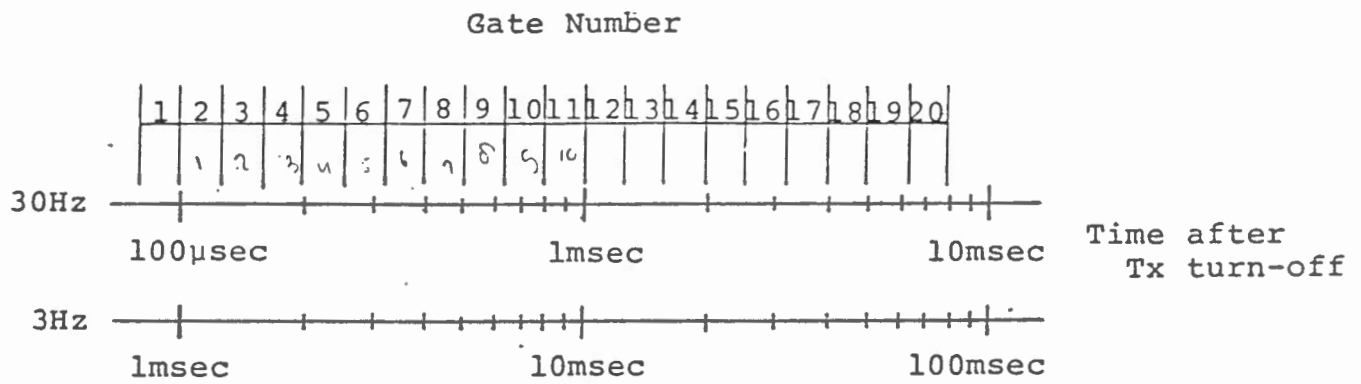
Receiver - Cont'd

Receiver batteries (continued) - battery weight 7.6 kg, 20 amp hour) or 2.5 hours continuous operating time (battery weight 2.6 kg, 6 amp hour). Two sets of batteries and a battery charger supplied to permit charging of spare set from transmitter motor-generator during survey.



Transmitter Current Waveform

FIG.A1



Gate Location and Widths (30 and 3Hz)

FIG.A2



EM31

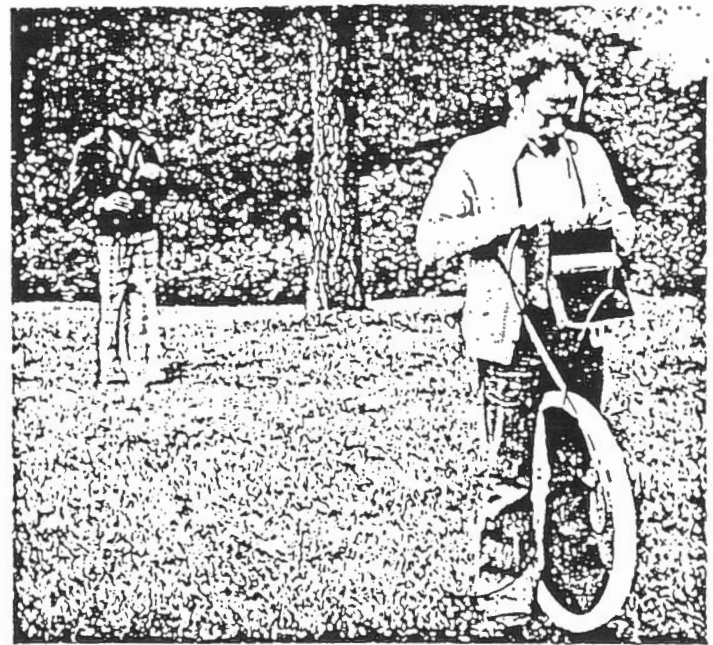
The Geonics EM31 provides a measurement of terrain conductivity without contacting the ground using a patented inductive electromagnetic technique. The instrument is direct reading in millimhos per meter and surveys are carried out simply by traversing the ground.

The effective depth of exploration is approximately six meters making it ideal for engineering geophysics. By eliminating ground contact, measurements are easily carried out in regions of high resistivity such as gravel, permafrost and bedrock. Over a uniform half space the EM31 reads identically with conventional resistivity and the measurement is analogous to a conventional galvanic resistivity survey with a fixed array spacing. Interpretation curves supplied with each instrument often permit an estimate of a layered earth.

The advantages of the EM31 are the speed with which surveys can be carried out, the ability to precisely measure small changes in conductivity, and the continuous readout which provides a previously unobtainable lateral resolution.

Specifications

MEASURED QUANTITY	Apparent conductivity of the ground in millimhos per meter.
PRIMARY FIELD SOURCE	Self-contained dipole transmitter
SENSOR	Self-contained dipole receiver
INTERCOIL SPACING	3.66 meters
OPERATING FREQUENCY	9.8 kHz
POWER SUPPLY	8 disposable alkaline "C" cells (approx. 20 hrs life continuous use)
CONDUCTIVITY RANGES	3, 10, 30, 100, 300, 1000 mmhos/meter
MEASUREMENT PRECISION	±2% of full scale
MEASUREMENT ACCURACY	±5% at 20 millimhos per meter
NOISE LEVEL	<0.1 millimhos per meter
OPERATOR CONTROLS	<ul style="list-style-type: none"> ● Mode Switch ● Conductivity Range Switch ● Phasing Potentiometer ● Coarse Inphase Compensation ● Fine Inphase Compensation
DIMENSIONS	Boom : 4.0 meters extended 1.4 meters stored Console : 24 x 20 x 18 cm Shipping Crate : 155 x 42 x 28 cm
WEIGHT	Instrument Weight : 9 kgm Shipping Weight : 23 kgm



EM34-3

Operating on the same principles as the EM31, the EM34-3 is designed to achieve a substantially increased depth of exploration and a readily available vertical conductivity profile.

The underlying principle of operation of this patented non-contacting method of measuring terrain conductivity is that the depth of penetration is independent of terrain conductivity and is determined solely by the instrument geometry i.e. the intercoil spacing and coil orientation. The EM34-3 can be used at three fixed spacings of 10, 20, or 40 meters and in the vertical coplanar (as shown) or horizontal coplanar mode. In the vertical coplanar mode, the instrument senses to approx. 0.75 of the intercoil spacing. In the horizontal coplanar mode, the instrument can sense to 1.5 times the intercoil spacing. For the horizontal coplanar mode, however, coil misalignment errors are more serious than in the vertical mode so greater care must be exercised to achieve the maximum 60 meter depth.

Simple operation, survey speed and straight forward data interpretation makes the EM34-3 a versatile and cost effective tool for the engineering geophysicist.

Specifications

MEASURED QUANTITY	Apparent conductivity of the ground in millimhos per meter
PRIMARY FIELD SOURCE	Self-contained dipole transmitter
SENSOR	Self-contained dipole receiver
REFERENCE CABLE	Lightweight, 2 wire shielded cable
INTERCOIL SPACING & OPERATING FREQUENCY	<ul style="list-style-type: none"> ● 10 meters at 6.4 kHz ● 20 meters at 1.6 kHz ● 40 meters at 0.4 kHz
POWER SUPPLY	Transmitter : 8 disposable "D" cells Receiver : 8 disposable "C" cells
CONDUCTIVITY RANGES	3, 10, 30, 100, 300 mmhos/meter
MEASUREMENT PRECISION	±2% of full scale deflection
MEASUREMENT ACCURACY	±5% at 20 millimhos per meter
NOISE LEVEL	< 0.2 millimhos per meter
DIMENSIONS	Receiver Console : 19.5 x 13.5 x 26cm Transmitter Console : 15 x 8 x 26cm Coils : 63cm diameter
WEIGHTS	Receiver Console : 3.1 kg Receiver Coil : 3.2 kg Transmitter Console : 3.0 kg Transmitter Coil : 6.0 kg Shipping Weight : 41. kg

EM37 Ground Transient Electromagnetic System
Technical Specifications

Transmitter

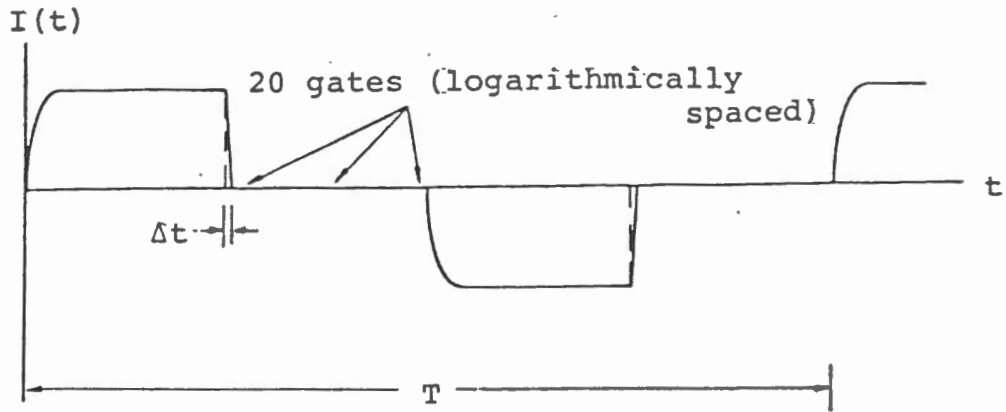
- Current Waveform - See Fig.A1
- Repetition rate - 3Hz or 30Hz in countries using 60Hz power line frequency; 2.5Hz or 25Hz in countries using 50Hz power line frequency; all four base frequencies are switch selectable.
- Turn-off time (Δt) - fast linear turn-off of maximum 300 μ sec. at 20 amps into 300x600m loop. Decreases proportionally with current and (loop area)^{1/2} to minimum of 20 μ sec. Actual value of Δt read on front panel meter.
- Transmitter loop - any dimensions from 40x40m to 300x600m maximum at 20 amps. Larger dimensions at reduced current. Transmitter output voltage switch adjustable for smaller loops. Value of loop resistance read from front panel meter; resistance must be greater than 1 ohm on lowest voltage setting to prevent overload.
- Transmitter protection - circuit breaker protection against input over-voltage; instantaneous solid state protection against output short circuit; automatically reset on removal of short circuit. Input voltage, output voltage and current indicated on front panel meter.
- Transmitter output voltage - 150 volts (zero to peak) maximum; 20 volts (zero to peak) minimum
- Transmitter output power - 2.8 kw maximum
- Transmitter wire supplied - 1800m. #10 copper wire PVC insulated with nylon jacket; transmitter wire contained on 6 reels (supplied); 2 reel winders supplied.
- Transmitter motor generator - 5 HP Honda gasoline engine coupled to 120 volt, 3 phase, 400Hz alternator. Approximately 8 hours continuous operation from full (built-in) fuel tank.

Receiver

- Measured quantity - time rate of decay of magnetic flux along 3 axes.
- Sensors - two air cored coils of bandwidths 11 and 50 kHz respectively; each 66cm dia.x4x5cm cross-section. Low frequency coil for general use, high frequency coil for shallow sounding.
- Time channels - 20 time channels with locations and widths as shown in Fig.A2. Successive operation at 30Hz, then 3Hz, effectively gives 30 channels covering range from 80 μ sec. to 80 msec.
- Output display - 4 figure digital LED plus sign; display also shows channel number and gain.
- Integration time - 2^n cycles at 30Hz; n=4,6,8,10,12,14 (switch selectable); similar integration times at other base frequencies.
- Receiver noise - approximately 1.5×10^{-10} volt/m²/turn of receiver coil at last gate at 30Hz with integration time of 34 seconds. Noise will be higher during intense local spherics activity.
- Output connector - all 20 channels available in analogue format from output connector at 5 volts fsd level.
- Synchronization to Tx - any of the following (switch selectable)
(1) reference cable
(2) primary pulse
(3) 27 MHz radio link (40 channels)
(4) high stability (oven controlled) quartz crystals.
- Noise rejection circuitry - with any of (1)-(3) above, entire system is automatically synchronized to 50/60Hz power line frequency when such interference exists in survey area; selective clipping of atmospheric noise pulses at all times. Audio output of Rx coil (transmitter pulse blanked out) is available on built-in loud speaker for ready identification of interference.
- Receiver batteries - 12 volt rechargeable Gel-cells; either 9 hours continuous operating time at 17°C (battery weight

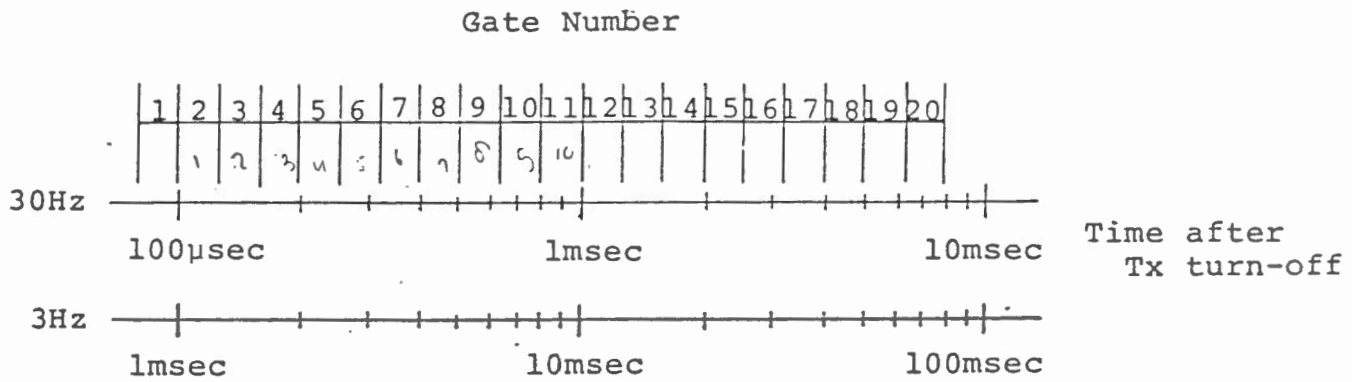
Receiver - Cont'd

Receiver batteries (continued) - battery weight 7.6 kg, 20 amp hour) or 2.5 hours continuous operating time (battery weight 2.6 kg, 6 amp hour). Two sets of batteries and a battery charger supplied to permit charging of spare set from transmitter motor-generator during survey.



Transmitter Current Waveform

FIG.A1



Gate Location and Widths (30 and 3Hz)

FIG.A2